Review Article

Institution of MECHANICAL ENGINEERS

Journal of MECHANICAL ENGINEERING SCIENCE

Proc IMechE Part C:
J Mechanical Engineering Science
2018, Vol. 232(22) 4128–4151

DOI: 10.1177/0954406217749869
journals.sagepub.com/home/pic

SAGE

# A review of electromechanical actuators for More/All Electric aircraft systems

**Guan Qiao[1], Geng Liu[1], Zhenghong Shi[2], Yawen Wang[3], Shangjun Ma[1] and Teik C Lim[3]**

## Abstract

Conventional hydraulic actuators in aircraft systems are high maintenance and more vulnerable to high temperatures and pressures. This usually leads to high operating costs and low efficiency. With the rapid development of More/All Electric technology, power-by-wire actuators are being broadly employed to improve the maintainability, reliability, and manoeuvrability of future aircraft. This paper reviews the published application and development of the airborne linear electromechanical actuator. First, the general configuration, merits, and limitations of the gear-drive electromechanical actuator and the direct-drive electromechanical actuator are analysed. Second, the development state of the electromechanical actuator testing systems is elaborated in three aspects, namely the performance testing based on room temperature, testing in a thermal vacuum environment, and iron bird. Common problems and tendencies of the testing systems are summarized. Key technologies and research challenges are revealed in terms of fault-tolerant motor, high-thrust mechanical transmission, multidisciplinary modelling, thermal management, and thermal analysis. Finally, the trend for future electromechanical actuators in More/All Electric Aircraft applications is summarized, and future research on the airborne linear electromechanical actuators is discussed.

## Keywords

Electromechanical actuator, testing system, fault tolerance, screw mechanism, power-by-wire

Date received: 9 May 2017; accepted: 24 November 2017

## Introduction

In recent years, there has been a trend in the aerospace field towards increasing the use of electrical actuation system that is usually called power-by-wire (PBW) actuation in the More/All Electric Aircraft (MEA/AEA).[1–4] The PBW technology seeks different design approaches and extends the applications of electrically powered actuators, such as flight control, landing gear, thrust vector control (TVC), and engine actuation system.[5–7] The electrical actuation system employing PBW actuators, such as electro-hydrostatic actuator (EHA) and electromechanical actuator (EMA) shown in Figure 1, transports the power in 'wires' between the devices instead of hitherto hydraulic pipeline, which remarkably improves the actuation performance of aircrafts.[8,9]

Studies have shown that PBW actuators will benefit actuation systems with a series of advantages due to their fault-tolerant capability and exclusion of pipes and fluids: (a) increased safety and reliability due to the absence of poisonous and flammable hydraulic fluids; (b) reduced weight, volume, and complexity of power transmission paths (Figure 1); (c) easier maintenance and less costs due to the lack of hydraulic leaks and better diagnostic capability; and (d) higher energy efficiency and better dynamic characteristics. These actuators are already found on in-service aircraft, in which EHAs and EMAs have become gradually mature enough to be introduced in recent large commercial transport aircrafts. For example, EMAs are used for landing gear braking, mid spoiler surfaces, and trimmable horizontal stabilizer on Boeing 787.[10] On Airbus A380, EHAs are already in service for primary flight controls (ailerons and elevators), while EMAs are employed for slats, trimmable horizontal stabilizer, and thrust reverser actuation.[11] On the military side, the Joint Strike

[1]Shaanxi Engineering Laboratory for Transmissions and Controls, Northwestern Polytechnical University, Xi'an, China
[2]Department of Mechanical and Materials Engineering, Vibro-Acoustics and Sound Quality Research Laboratory, University of Cincinnati, Cincinnati, USA
[3]University of Texas at Arlington, Arlington, USA

**Corresponding author:**
Geng Liu, Northwestern Polytechnical University, No. 127 Youyi West Road, Beilin District, Xi'an 710072, China.
Email: npuliug@nwpu.edu.cn

Fighter has been equipped with EHA-actuated primary flight control systems. The actuator engineers estimated[12–14] that PBW actuators and related electrical systems could achieve a significant reduction in the fuel burn and maintenance costs on an all-electric passenger plane and lead to a 30–50% reduction of the ground service equipment. For military aircraft in combat situations, the take-off weight could be cut down by 600–1000 lb, and the vulnerability of the fuselage area could be reduced up to 14%.[15,16] Although PBW actuators are still relative new to the aerospace industry, the concept of MEA/AEA offers more significant opportunities for PBW actuators in the future.

As shown in Figure 1(a), the EHA is basically a self-contained hydraulic actuator incorporating a pump driven by a variable speed electric motor. In contrast to the hydraulic system, the power control is done by the pump. Varying the flow and thus the hydraulic power is achieved by changing the pump's speed. By transferring back and forth the fluid from one cylinder chamber to the other, the electric motor and pump assemblies could control the position of the piston connected to the load. As a result, the bulky piping systems and external hydraulic source are eliminated.[17] Conversely, EMAs allow the elimination of local hydraulic devices and do not use the hydraulic flow to drive the screw rod, which leads to a significant maintenance reduction due to less energy conversion and provides a better option for leak-free operation.[18] It is generally accepted that when sized for the same actuation requirements, the EMAs have a weight advantage over the EHAs.[19] In spite of the above advantages, researchers and engineers still face new challenges in the development of EMA technologies for future aircraft applications. Unlike conventional hydraulic servo actuators (HSAs), the principal problem in the extensive application of EMAs is the

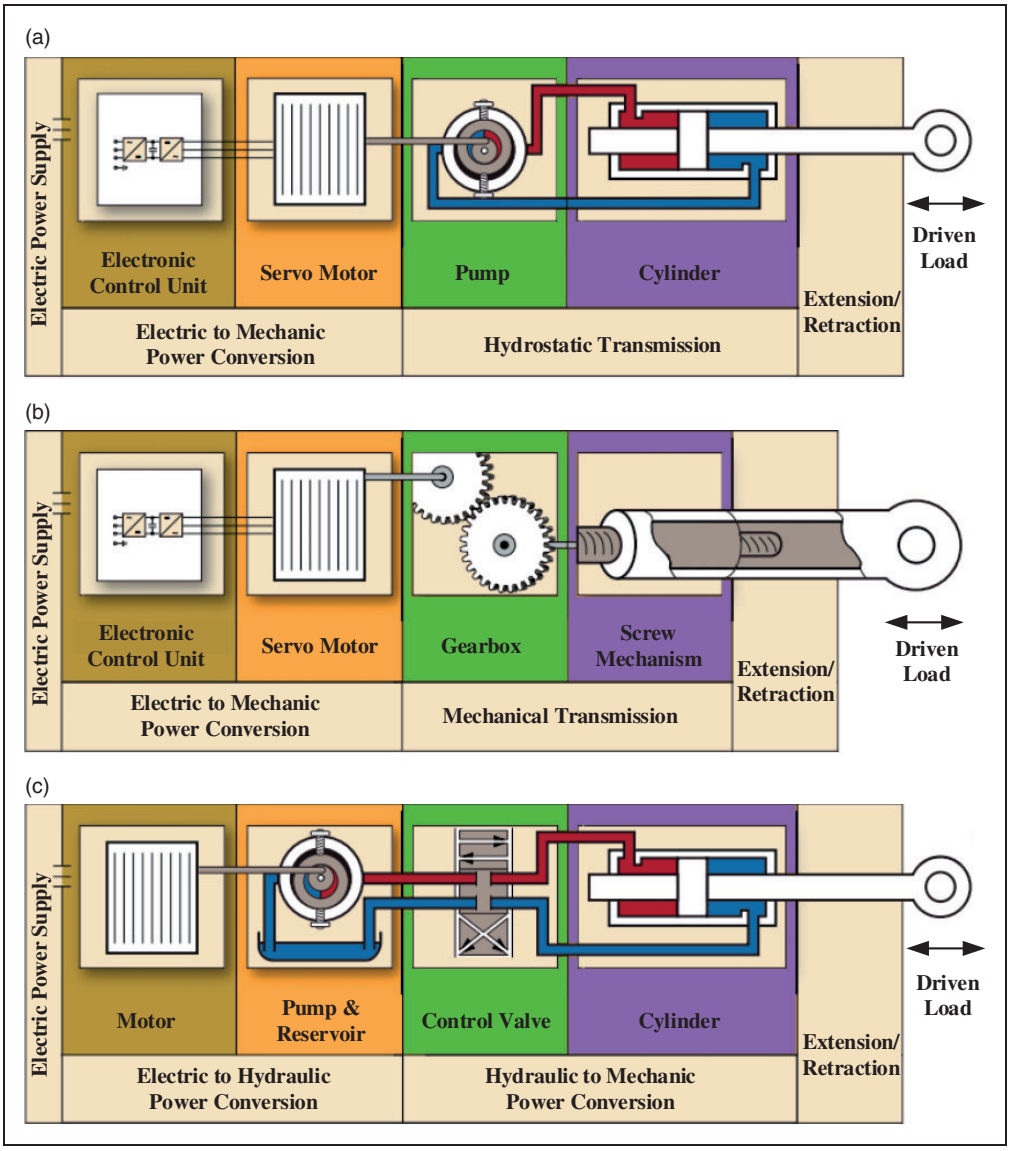


**Figure 1.** Power-by-wire actuators and HSA composition. (a) EHA, (b) EMA, and (c) HSA.

lack of accumulated knowledge and experience regarding reliability and the risk of failures due to jamming, health monitoring (HM) and assessment, and thermal management. To ensure the required performance of airborne EMAs, detailed experimental tests must be implemented for their characterization and validation.[20]

This study reviews the development of the linear EMA system and its testing system, with special regard to the flight controls. First, four different applications of airborne EMAs on MEA/AEA systems are primarily taken into consideration, with major efforts on research and development projects. Second, two typical forms of EMAs and their characteristics are analysed to have a better understanding of the different architectures and mass distributions. Third, an exhaustive review on various EMA testing systems is presented, including performance testing equipment and methods based on room temperature, thermal vacuum environment, and iron bird. Furthermore, common problems and tendencies of the testing systems are revealed. Fourth, key technologies and research challenges on airborne EMAs are discussed in terms of fault tolerance, reliability, system modelling methods, and thermal management. Finally, some potential tendencies of linear EMA development are discussed in future PBW aircraft applications.

## Background review

The EMA can be either linear or rotary type. For linear EMAs, the rotational motion of the motor is transformed into the linear motion by a mechanical assembly, such as a ball or roller screw mechanism. For rotary EMAs, the motor speed is reduced by a gearbox, which is connected to the surface either directly to the hinge line or by a connecting rod assembly.[21] Figure 2 shows the major components of and differences between linear and rotary EMAs. As a more general application, the linear EMA in the aircraft application is mainly considered and discussed in this study.

### Development and application

The maturation of More/All Electric solutions conducted in the laboratory environment can take several decades before operating in mission conditions. Technology Readiness Levels (TRLs) are used to identify the maturity of a new technology, from TRL 1 (basic scientific research) through TRL 9 (being put into service for a larger system). For example, the EHAs took about 30 years from the initiation of technology concept on mid-1980s to the application on Airbus A380 in 2007. The EMAs follow the same path in the different domain. The first development in space applications stimulate the EMA's advance from the 1970s,[23,24] and it is also found their functionality on the Space Shuttle, X-38 Crew Return Vehicle,[25] and unmanned aerial vehicle[26] flight controls. This review places extra emphasis on their electrical actuation solutions for commercial aircrafts and helicopters. On a MEA/AEA, power requirements and functional characteristics for actuation are numerous and different. They essentially concern the following applications.

*Primary flight controls.* The purpose of primary flight controls is to control aircraft trajectory, i.e. to control the three rotational degrees of freedom: the ailerons

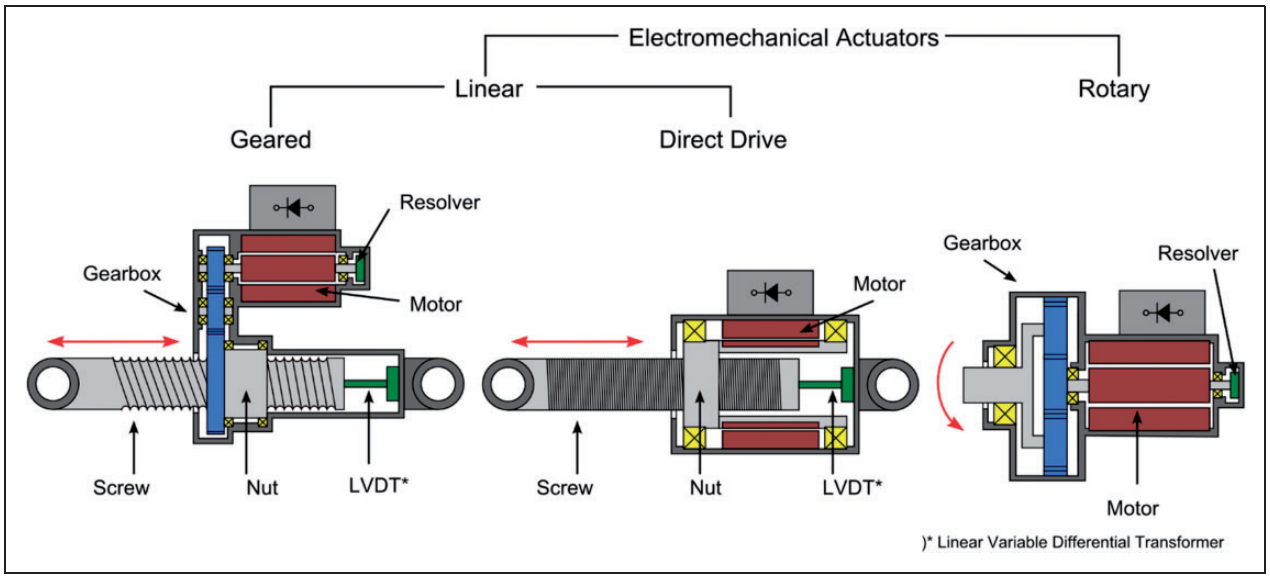


**Figure 2.** Classification of different EMA types. This figure was adapted from Figure 1 of Wagner et al.[22] with the permissions from the copyright owner SAE International.
LVDT: linear variable differential transformer.

for roll, the rudder for yaw, and the elevator for pitch (Figure 3). Until the 1980s, the experiences of EMAs used for primary flight surface control were increased, and many aircraft manufacturers and researchers began to test and verify EMAs. To establish credibility for the EMA technology and to obtain practical experience, a dual linear EMA for controlling the left aileron of a C-141 aircraft was developed and demonstrated for flight test in 1986 instead of the dual HSA.[28] Encouraged by the successful results of the C-141 aileron, additional PBW systems in a variety of sizes and configurations were further developed. Beginning from 1990, Lucas Aerospace[9] fabricated the flight quality EMA demonstrators for large aircraft aileron, which was the first system designed to be used for a primary flight control surface. The system advances include the development of stress-limiting device and damping generator to prevent flutter in the event of system shutdown. Besides, development programmes have been conducted to validate their feasibility in terms of new technology and to demonstrate their integration within the flight control surfaces. Such research activities that have been completed involve EMAS,[29] EPAD,[30] and MOET.[31] It is noteworthy that the foundation for EMA characterization originates from the experiments in the EPAD project, where a HSA of the left aileron was replaced with a duplex EMA. The EMA comprised two 3-phase brushless direct current (BLDC) motors to drive a single ball screw through a differential gearbox. The introduced gearbox was used to sum the output velocities of the individual motors, thus eliminating force fighting between two lanes. The thermal performance of the EMA was highlighted, where the worst thermal loading occurred when the aircraft deployed the ailerons as flaps, flying around for extended periods of time. The extended operation against a steady load, coupled with the continuous small corrections at slow speeds, resulted in the termination of a test point. The main characteristics of EMAS and EPAD projects are provided in Table 1. In the frame of the COVADIS project,[33] a civil aircraft A320 successfully flew an EMA on its right aileron surface for the first time. Thereinto, 114 flight hours and 38 flight cycles were accumulated without any alarm occurred, which means a good level of TRL6 has been achieved. Between 2011 and 2016, the Actuation 2015 project aimed at developing and validating a common set of standardized and scalable EMA modules that addressed cost, reliability, and weight requirements.[34] The actuation systems included primary and secondary flight controls on large commercial aircrafts as well as helicopters.

As for helicopters, the flights are controlled by acting on the swashplate and on the collective pitch of tail rotor blades. Within the HEAT programme,[35] an electromechanical actuation system was developed to address rotorcraft relevant issues by reducing the

**Table 1.** Characteristics of EMAs in EMAS and EPAD projects.

| Project | EMAS | EPAD |
|---|---|---|
| Date | 1985–1986 | 1990–1992 |
| Aircraft and application | C-141/Aileron | F/A-18/Aileron |
| Flight test hours | 12.5 | 25 |
| Blocked force (kN) | 84.7 | 53.65 |
| No-load speed (mm/s) | 118 (motor 9600 r/min) | 214 |
| Stroke (mm) | 138 | 112.8 |
| Output backlash (mm) | 0.45 | 0.51 |
| Mass (kg) | 29.5 | 12.5 |
| Bandwidth (Hz) | 4 | 7 |

Source: This table was adapted from Table 6.3 of Mare[32] with the permissions from the copyright owner John Wiley and Sons.
EMA: electromechanical actuator.

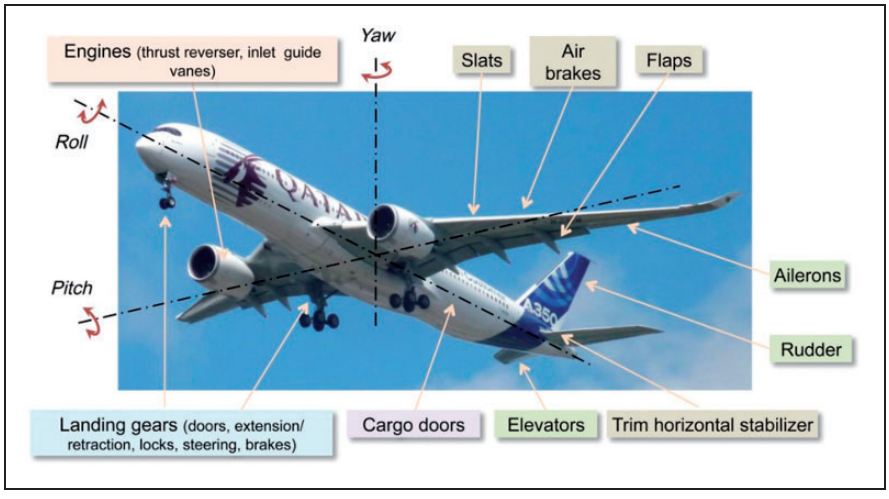


**Figure 3.** Different actuation needs on a commercial aircraft. This figure was adapted from Figure 1.2 of Mare[27] with the permissions from the copyright owner John Wiley and Sons.

possibility of jamming in mechanical transmission components. At the beginning of 2010, the HEMAS project[36] was restarted to demonstrate the technology to TRL5. Furthermore, for the potential EMA's application to individual blade control (IBC), Project Zero[37] successfully built a hardware to use IBC as the primary flight control in a tilt rotor aircraft. Although all these research activities and development efforts, EMAs are not yet mature enough for primary flight controls because of their jamming probability except for low-power applications. It is acknowledged that EMAs for primary flight control applications face a long way from aviation acceptance as safe.

*Secondary flight controls.* There appears higher acceptability for manufacturer of EMA-actuated surfaces in less safety-critical applications, such as flaps, slats, spoilers, and trim horizontal stabilizers. These are surfaces where jamming is not catastrophic and operated discontinuously. The high lift actuation system controls the slat and flap surfaces to increase lift during take-off and landing. Developed between 2001 and 2004, the DEAWS research project[38] was a typical demonstrator to investigate the feasibility of high lift systems distributing electrical actuators for reducing system complexity. Initial tests on the motor and power electronic converter, and symmetry control tests between flap surfaces were performed on an industrial test rig. When an actuator failure appeared, DEAWS allowed the failed surface to lock a position, but maintained operation of the remaining surfaces. As for spoiler actuations, Fronista and Bradbury[39] developed an EMA on a spoiler for a transport aircraft, where an incorporated ratchet mechanism was to remain the spoiler surface in that position in case of power loss. At the in-service level, the EMAs were already served on the advanced Boeing B787 for four out of 14 spoilers (Figure 4). It is also worth noting the first full electrically powered Trimmable Horizontal Stabilizer Actuator was implemented on the A350,[40] which represents a major advance for the secondary flight control actuation system.

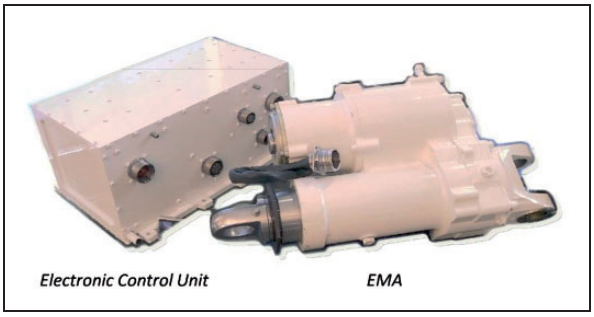


**Figure 4.** Spoiler EMA used in Boeing B787 and its ECU. This figure was adapted from Figure 6.4(b) of Mare[32] with the permissions from the copyright owner John Wiley and Sons. EMA: electromechanical actuator.

*Landing gears.* The requirements of actuation functions in landing gears are numerous, including raising or lowering of landing gears (extension/retraction), nose-wheel steering, and wheel braking. Since the control of the extension/retraction is simple, the main difficulties focus on the tolerance or resistance to jamming and the ability of damped free fall in case of function loss. This is the reason why most research programmes ELGEAR,[41] CISACS, and MELANY[42] discussed about the testing and evaluation of jamming-related efforts when the extension/retraction is actuated by EMAs. In 2005, the DRESS project[43] aimed to develop and test a highly reliable electromechanical nose gear steering system for a single aisle commercial aircraft. Afterwards, an electric landing gear system in ELGEAR NWS project[38] was developed between 2007 and 2009. It was found that the frequency response of the actuator was limited by the considerable backlash in the mechanical system. The temperature monitoring proved a major failure, thus a free-to-castor mechanism was employed to resist actuator jams. The EMA braking is achieved by applying high axial force on the pack, which eliminates the hydraulic fluid in the severe condition and facilitates maintenance. As an example, the EABSYS project (launched in 1999)[44] involved EMAs to apply the wheel brakes of an aircraft and demonstrated the EMAs can operate a brake system after the actuator jamming. For the in-service application, a total of 32 EMAs and four motor control electronic units have also entered service on Boeing B787.

*Engines.* The EMAs used for MEA/AEA engines also perform numerous control and monitoring functions, such as variable stator vanes and variable bleed valves steering, thrust reversers control, and geometry modification of air intakes or nozzles.[45] Although the duty cycle of these actuators is relatively short, they are characterized by working under harsh operating environment (temperature from $-50$ to $+125\,^{\circ}\mathrm{C}$, high stresses of up to 60 kN). It has proven that roller-screw-based EMAs performed gate actuation of the engine air intakes with no failures throughout the service life of the supersonic airliner.[46] Recently, Airbus A380 and A350 introduced EMAs in their Electric Thrust Reverse Actuation System.[40] Mechanical power was distributed by flex shafts to the central actuators, and then transmitted the motion and force to the transcowl. For the thrust reverser's application, the synchronization of EMAs is the crucial consideration.

## Architecture of EMA

The EMA (Figure 5) generally consists of a mechanical actuation assembly (namely actuator module, including mechanical components and a servo motor) for converting electric energy into mechanical energy and an electronic control unit (ECU) for

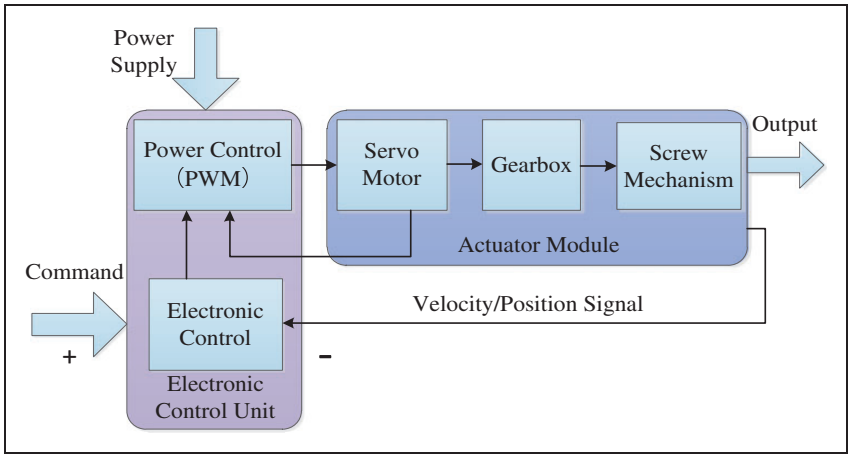


**Figure 5.** Gear-drive EMA schematic.

power and signals. Their functions and characteristics are described as follows:

(a) **Servo motor**

A compact variable-speed servo motor with high reliability, high power density, and acceptable heat dissipation is required in flight control case. Several motor types may be suitable, and three common options are permanent magnet synchronous motor (PMSM), BLDC motor, and switched reluctance (SR) motor. The choice of motors normally depends on the power supply on board. For example, the PMSM can be an appropriate type when an alternating current power supply directly drives a servo motor.[47] The motor controller is used to control the speed and direction by windings' electrical switch through power electronic devices. An empirical mass estimation of a BLDC motor and its power electronics based on torque–speed characteristics can be referred to Torabzadeh-Tari.[48]

(b) **Gearbox**

The main purpose of the gearbox is transforming the servo motor's high speed and low torque to low velocity and high torque of a screw mechanism. Harmonic gear reducers, cycloidal reducers, or planetary gear reducers are an effective option because of their compact structures, ease of reaching zero backlash, and high efficiency. It must be noticed that a major part of the actuator mass can be devoted to the servo motor when using planetary gear reducers due to their low transmission ratio, compared with the high reduction ratios of harmonic and cycloidal reducers.

(c) **Screw mechanism**

Either a ball screw mechanism (BSM) or a planetary roller screw mechanism is used to convert the rotary motion to linear motion with a required force. Connecting the servo motor and external load, torque and speed are matched by the transitional mechanism. For a given load, the planetary roller screw mechanism is made with a lower lead than the BSM and its load capacity is higher. Total mass of the actuator tends to decrease when the transmission ratio increases by increasing the reducer transmission ratio and decreasing the lead of the screw mechanism.[49] To maximize stiffness while minimizing weight, a hollow screw shaft is selected to accommodate a linear variable differential transformer to measure the screw rod's linear position for control loop closure.

(d) **ECU**

The EMA module is controlled by a suitable ECU, which works at 28 Vdc power from a power supply. Power control determines motor current by voltage pulse width modulation to the motor in response to a position or torque command signal. The EMA position and load sensor send the position/velocity and load information to the ECU for position feedback and current limitation. For flight status where the external load is high, additional temperature sensors are usually installed on the controller housing near the connectors to record the external temperature rises and to alarm high temperature.

Actuator weight shall be permanently challenged during the preliminary and detailed design phase. At the actuator level, each component can have a significant impact on the parameter criteria as the total mass depending on the mission profile and architecture configuration.[50] Figure 6 shows the mass distribution of the EMA components using scaling laws[52] to perform an automated preliminary sizing. Although the difference is objectively existed and permitted between the components standardization of a product range and the calculated optimal configuration, it is still critical for sizing calculations with limited input parameters and early simulations to mitigate risk.

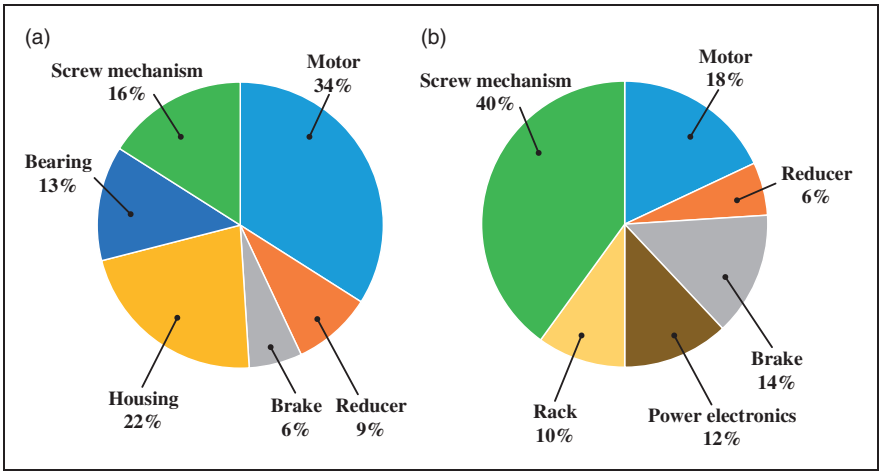


**Figure 6.** EMA mass distribution for (a) spoiler control (overall transmission ratio of 6283)[51] and (b) nose landing gear steering (overall transmission ratio of 2349).[50]

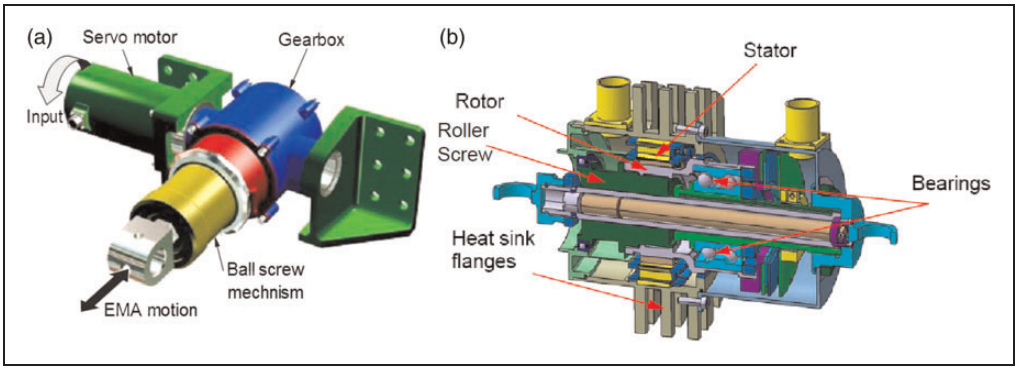


**Figure 7.** (a) Gear-drive EMA for high-power flight controls[5] and (b) direct-drive EMA model.[53] EMA: electromechanical actuator. (Courtesy of SAAB AB and SPAB.)

The EMA structure described by Botten et al.[5] for high-power flight controls is shown in Figure 7(a). As a basic form, the gear-drive EMA is susceptible to certain single-point failures[54] that would generate an undesired mechanical jamming, consequently bringing complications for flight certification on some surfaces. For these reasons, the gear-drive EMA is not suitable for primary flight control applications; nevertheless, secondary actuation systems and other actuation functions which are lower risk compared with flight control surfaces could accommodate such a technology. As an example, Wachendorf et al.[55] presented an actuation system that included two differential gearboxes with three shafts, incorporating two active-parallel operating load paths to control the stabilizer. Torque difference between the dual load-path EMAs (position summing via a differential gearbox in each path) can be compensated by one of the input shafts. In case of failure, the mechanical self-synchronization guarantees the free moving of both actuators.

The other common form is the direct-drive EMA, which includes a power converter and a high-power density motor that is directly connected to a screw mechanism without a gearbox. In this way, permanent magnet can be glued directly on the surface of the cylindrical nut that represents the rotor, thus leading to a correspondingly concentrated weight. Directly supporting the load, the screw mechanism is installed parallel on ball bearings so that the nut is connected to the housing for space saving. The direct-drive EMAs have the following advantages[56]: decreased mechanical jamming susceptibility, less probability of actuator damping loss, increased actuator efficiency and reliability, and reduced system inertia due to the elimination of the in-between gearbox. It could be a major improvement depending on the system acceleration requirements or the duty cycles. As a result, a high-performance servo motor is required with high torque density and reliability. On the other hand, in absence of gear transmission's buffering effect, any load disturbance or parameter perturbations can be directly reflected to the motor and the control system.[57] This architecture produces challenges to the control strategy for high load disturbance rejection ability and positioning precision. As for the direct-drive EMA that is based on the inverted roller screw technology, the difficulties of integrated manufacture are focused on the partial assembly and

accurate machining of long internal threads of the screw mechanism. Figure 7(b) demonstrates a direct-drive EMA model that a group of heat sink flanges are set outside the housing[53] because of the possibility of overheating.

Besides the above subcomponents, other power management functions such as clutch, brake, and torque limiter can be combined with the two basic architectures to accomplish flight surface motion. For example, to avoid damage to other components, a torque-limiting device is used as a backup limitation system in the event of electrical load limitation failure. Coupled and uncoupled through a command signalling directly from the ECU, a friction-type clutch can also be incorporated into the drive train to manage mechanical power. Also, a gear-drive EMA that is equipped with a brake motor could enhance the power density, and therefore, braking energy can be recycled.[58] However, overall costs and weight will also rise due to the increased complexity of the system.

## EMA testing system

Even though the EMAs have been correctly designed and implemented, feedback from the experimental testing is needed, for a better understanding of various faults and operating characteristics under varied working conditions. More generally, a testing process from universality to particularity would commonly be adopted to examine the EMA's capacity and reliability. In this work, testing systems in three conditions include room temperature situation, thermal vacuum environment, and iron bird, which are elaborated and summarized to guide the EMA testing system design.

### *Testing system at room temperature*

In the early 1990s, PBW actuation testing systems including the EMA system have been established at room temperature. Schinstock and Haskew[59] designed a dynamic load test stand to yield a large dynamic load on a test EMA. The test stand utilized high-bandwidth hydraulic actuation to generate heavy loads on a roller screw mechanism for evaluating the effects of large, high frequency loads on the mechanism. This equipment demonstrated a simple I-beam structure with a limited working range. The qualification of EMAs requires relevant ground testing in accordance with the operating conditions. In such an attempt, Mare[60] designed an actuator test stand to assess the actuator closed-loop dynamic characteristics and its endurance capability. With a vertical architecture in Figure 8, the test stand could simulate in-flight operating conditions of helicopter actuators and launcher thrust vector actuators. It can also represent the structural stiffness of airframe and the inertia of actuated load. Gravity compensation can be also added, if necessary. An active loading system design ensured a high load and high performance

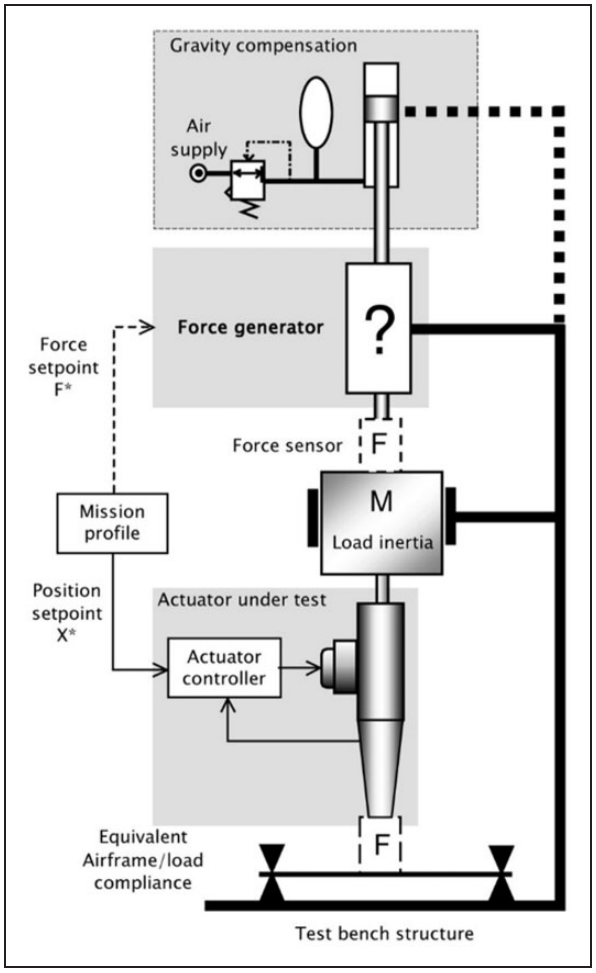


**Figure 8.** Vertical structure of actuator testing system. This figure was adapted from Figure 1 of Mare[60] with the permissions from the copyright owner Emerald Group Publishing Limited.

expectation, but it is difficult to ease the possibility of interaction with a test actuator. Similarly, a servo actuation evaluation system was established to investigate the influence of friction and clearance in transmission mechanisms, simulated rudder inertia, and anchorage stiffness on the actuator performance. The test rig (Figure 9(a)) was considered as a horizontal closed-linear structure to guarantee the rigidity of actuator's installation in different sizes. With a single variable factor or combined factors of the stiffness, inertia, friction, and clearance, the impact of those factors on EMA static and dynamic performance, such as step response, frequency response, and dynamic stiffness testing can be performed.

For seeded fault testing, Smith et al.[62] performed an experimental research on EMA faults and a data-driven diagnostic approach including experimental test stand build and model-based HM. According to the system requirement, a full-scale EMA test stand was established in the experiments for validating fault analysis and prognostics algorithms. Several critical failure modes, such as backlash, BSM jamming, shaft eccentricity, winding short, and resolver fault

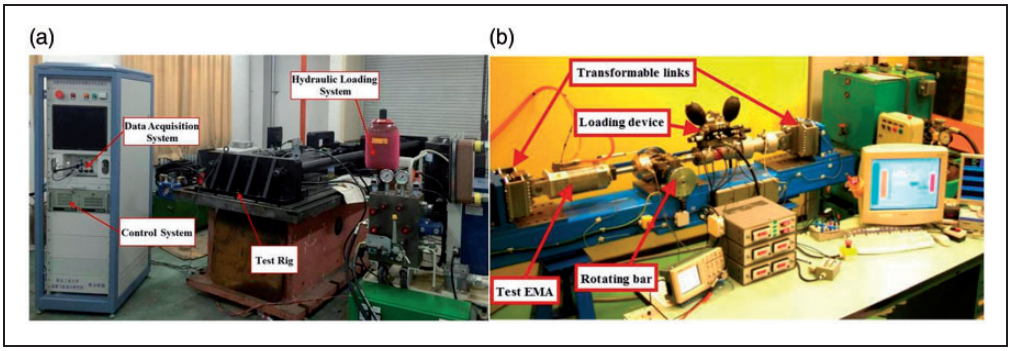


**Figure 9.** (a) Evaluation system of servo actuation system and (b) EMA testing system in Toulouse.[61]

**Table 2.** Health management systems of EMA.[62]

| Item | Test method | Test range |
|---|---|---|
| Position response of EMA when loaded | An magnetostrictive linear position sensor is connected to the coupled actuators by a mounting plate to monitor the system motion. | Maximum speed is 208 mm/s and stroke lengths is up to 450 mm. |
| Backlash of screw mechanism during repeated motion | A non-contact laser interferometer is used to observe the backlash event. | The entire range of measurement is 50 mm; resolution of relative motions is 0.001 mm. |
| Actuated load | An in-line load cell with compressive and tensile capacity is attached to the coupled actuator shafts and provides system feedback. | The custom loading profiles is up to 5 metric tons. |
| Drive current in the motor windings | An internal current sensor within the T200 series servo drive is recorded by the data acquisition system as an indication of the motor torque. | N/A |
| Vibration measurement | Some accelerometers are located on the centreline of the bottom surface of the actuator housing to indicate the EMA bulk vibration. The others are mounted near the two topmost ball return channels inserts to measure the vibrations of the ball-screw nut assembly. | N/A |
| Temperature of motor and ball screw mechanism | Type T thermocouples are attached to the inside of the motor housing near motor windings and internal ball-screw nut surface. | N/A |

EMA: electromechanical actuator.

were inserted into the EMA,[63] and some of the test methods and ranges are listed in Table 2. The loading system could create customizable force by a larger load EMA instead of hydraulic or pneumatic systems. The test EMA was equipped with some sensors that provide a high-precision representation where a laser sensor was used to observe the backlash over a shortened stroke. Data acquisition software was executed on the central computer and provided the user with interface for system monitoring, testing case, and data visualization. In addition, other typical testing systems are summarized in Table 3.

Other researchers also designed and built relevant actuator testing systems and conducted many tests[71–74] including dynamic stiffness, vibration, temperature, and matrix converter experiments to expedite the validation of EMAs at room temperature. From the above statements and analyses of different actuator testing apparatuses, some facts about the EMA testing system are summarized and noted:

1. The testing parameters of EMA performance assessment include various measured data such as force, velocity, position accuracy, motor current, temperature, vibration, frequency response, and dynamic stiffness. Also, it is highlighted that the testing system should provide a function of fault diagnosis and reliability detection in fault injection experiments to characterize the EMA performance by these parameters. The requirement of fault testing on the system components contributes to a successful development of airborne EMAs.

**Table 3.** Examples of some typical EMA testing systems at room temperature.

| | | |
|---|---|---|
| Karam and Mare[61,64] | Application and purpose | Design non-intrusive experiments to identify model parameters of inverted-roller-screw based EMAs |
| | Layout and component | A horizontal standard actuator test bench (Figure 9(b)), including:<br>(i) A test EMA;<br>(ii) A hydraulic actuator as the loading device;<br>(iii) A rotating bar (constant load inertia of 1 kg $\times$ m$^2$), and transformable links (constant airframe stiffness of $1.4 \times 10^7$ N/m);<br>(iiii) Non-intrusive sensors to measure the force, pressures, and the rod-to-body extensions; |
| | Test items | (i) EMA stiffness test by using active and passive method;<br>(ii) Blocked/moving load and time/frequency domain experiments for developing the progressive model of mechanical energy losses and system inertia; |
| | Feature and limitation | The test EMA or load actuator can be passivated or controlled either as a position or a force generator;<br>Allow multiple purposes such as force fighting study;<br>Variant installation conditions such as the structural stiffness and inertia is not considered; |
| Koopmans et al.[65]<br>Ismail et al.[66]<br>Zhang et al.[67] | Application and purpose | Diagnose EMA faults and employs prognostic algorithms to predict the actuator's remaining useful life (RUL) for aerospace applications regarding critical failure modes |
| | Layout and component | A scaled-down portable test stand fitted inside a standard 19″ rack;<br>(i) Chassis assembly: all support structures;<br>(ii) Power assembly: a standard power supply for all power inputs;<br>(iii) Central processor assembly: includes PC, data acquisition, motor drivers;<br>(iiii) Actuator coupling assembly: includes one load and two test actuators; |
| | Test items | (i) Create hundreds of fault scenarios using position and load profiles, and fault magnitude levels;<br>(ii) Conduct run-to-failure experiments to validate the RUL prediction based on different algorithms;<br>Use vibration-based hybrid technique for detecting the jam fault and screw spall; |
| | Feature and limitation | A lightweight, self-contained test stand that can support different actuators;<br>Allow test actuators to be subjected to realistic environmental and operating conditions, but the profile of displacement and load are scaled down;<br>Deficient validation procedure under the same conditions; |
| Tursini et al.[68]<br>Castellini et al.[69]<br>Antonelli et al.[20] | Application and purpose | Use an Automatic Test Equipment (ATE) to verify the cooperative working of the Twin EMAs to drive the flap surfaces |
| | Layout and component | (i) PC panel: host PC controls the hydraulic actuator generating realistic load profiles;<br>(ii) Drive panel: contains the control system, the DC power supply, and two fault-tolerant inverters;<br>(iii) Testing bench: EMAs are linked by a stiff plate while a hinge connects the plate to a truck. A hydraulic actuator is connected to the truck; |
| | Test items | Evaluate the system response (position profile, maximum speed, current, and force) with (i) two EMAs, (ii) a fault in one or two phases of an EMA, and (iii) an EMA out of service; |
| | Feature and limitation | Adopt a multithreading approach to satisfy mandatory time constraints;<br>Results are recorded in the NI TDMS format for an off-line analysis;<br>The hydraulic circuit had difficulty in following the imposed profile;<br>Not easy to test different size of EMAs; |
| Legrand et al.[70] | Application and purpose | Actuation system performance tests in accordance with A320 Aileron actuator specification |
| | Layout and component | (i) A force controlled antagonist jack is used to load the EMAs;<br>(ii) Two EMAs are installed in duplex arrangement, which allows active/damping management; |

(continued)

**Table 3.** Continued

| | |
|---|---|
| Test items | (i) Motor Drive Electronics tests on AC/DC electrical networks;<br>(ii) Health monitoring of electric and mechanical components based on a Fault Anticipating System;<br>(iii) Optimized roller screw endurance test; |
| Feature and limitation | Representative of the aircraft in term of inertia, kinematics, and stiffness;<br>Influence of mechanical friction and backlash on EMAs cannot be obtained; |

EMA: electromechanical actuator.

2. The linear actuators are typically tested against the conditions existing in the substantive service. In order to test the above parameters, the test stand must be representative of the structural stiffness and inertia of the airframe, equivalent mechanical friction loss, and backlash requirement, according to the system requirement.
3. The test and load actuators are mostly in line/parallel with each other (horizontal, vertical, or compact architecture), where the load one can be of different types including pneumatic, hydraulic, and electromechanical. The EMA's stroke is regarded as a disturbance to the load actuator as it attempts to provide an appropriate force, and the loading force is also seen as a perturbation to the stroke. This prominent technical difficulty is called superfluous force, which can be mitigated by general velocity feedforward compensations or adding a flexible mechanical buffer between the two actuators.
4. The data acquisition software provides the user interface for testing case definition, motion or force control, data visualization, and post-processing. The control system should have a function of giving warnings and alarms to alert the users in unsafe or undesirable situations, and even shut down all test stand runs.

### *Testing system in a thermal vacuum environment*

The test process in a thermal vacuum environment ensures the reliable use of EMAs in some flight environments. For example, the EMAs were certified on flight test vehicles in a qualification test procedure.[25] The procedure was operated on a spring stand (as well a thermal/vacuum chamber). The testing result indicated that the EMAs were simple to use and had minimal risks to ground operations. In 2014, Barnett[75] constructed a laboratory apparatus and data acquisition system for evaluating aircraft flight control actuators using an environmental chamber to simulate actuator bay temperature. Key performance characteristics, such as frequency response, step response, reversal, backlash, and holding, were carried out to validate that this set-up could successfully evaluate and characterize EMAs. The actuator was placed in an environmental chamber (Figure 10) that duplicates the ambient temperature as a function of altitude. It can generate desired heating and cooling rates commonly found in an aircraft envelope. The apparatus could record EMA electrical, mechanical, and thermal parameters synchronously, which provides a basis for energy analysis.[77] The EMAs used for CleanSky HP-SMART EMA project[78] were qualified in vibration and thermal tests. It was suggested to implement a speed limit in the control system that varies as the temperature decrease to avoid high current consumptions.

Currently, the loading system in a thermal vacuum environment mainly includes the spring loading and hydraulic loading method. Nevertheless, the spring loading is a generic passive loading that has some limitations when high-frequency load is needed. The thermal vacuum environment is achieved by putting the test EMA or overall aircraft into an environmental chamber with hot or cool air injection. For example, Kudlac et al.[79] described a thermal vacuum facility that provided thermal vacuum simulations to support lightweight structures testing. A vacuum level of $1.3 \times 10^4$ Pa and a uniform temperature environment of approximately 77 K were accomplished in the vacuum chamber. Meanwhile, a nominal heat flux of $1.4\,kW/m^2$ in the chamber's interior was formed due to the infrared lamp array, which simulates radiation to space and solar exposure on the aircraft surface.

### *Testing system on iron bird*

For any actuation type, the iron bird testing is intended to validate the coupling of the EMAs with other systems. In the previous flight test experience,[30] the EMA system was built in a hardware-in-the loop test stand, which simulated the assembly position and kinematics of the aileron. The avionics were integrated on a retired iron bird. This set-up was used to perform system verification, performance validation, and contrastive testing, such as position and frequency response. Test results showed that the EMA slightly outperformed the standard actuator on the right aileron in terms of tracking capabilities. However, the thermal performance of the EMA was worse, and the maximum thermal response was up to 110 °C. Constant aero loads required the servo motor to maintain constant torque causing high current

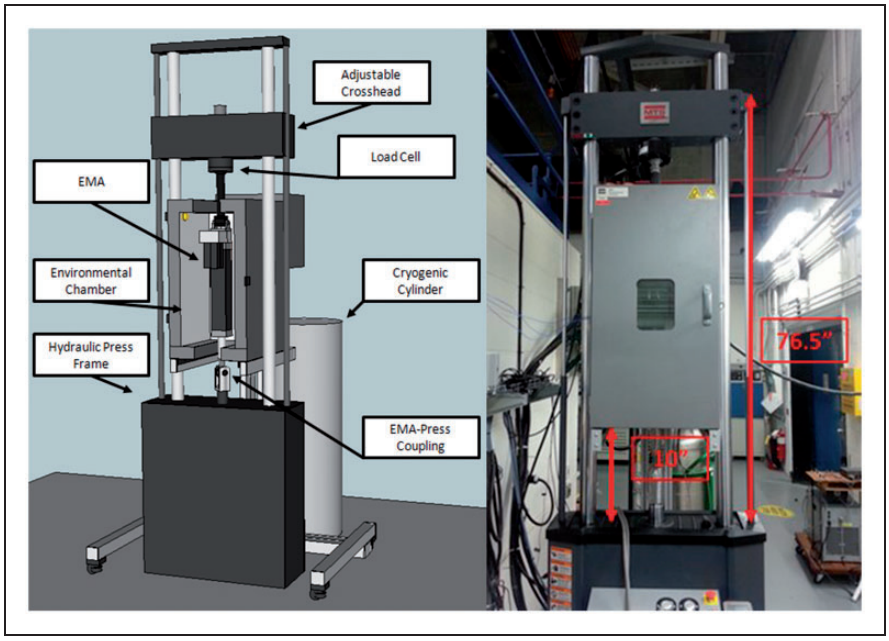


**Figure 10.** Thermal vacuum environmental test apparatus.[76] EMA: electromechanical actuator.

draw and heat generation due to winding resistance.[80] Further to an iron bird testing of the EMAs in COVADIS project,[81] a clearance for flight was obtained based on the qualification tests. Regarding to prognostic experiments on helicopters, Balaban et al.[82] reported that a flyable EMA test bed was mounted on the floor of the aircraft cabin to initially validate the diagnostic and prognostic method. During the tests, the load profiles were derived using the real-time flight data and the timescale of fault growth was within the duration of a single flight.

In addition, iron bird testing was expected to verify the coupling of the PBW actuators with the electrical generation, using torsion bars[83] to reproduce the aero loads at each actuator. The testing showed that unrealistic harsh surface movements, such as frequency response, can be harmful under these loaded conditions. However, this iron bird thermal environment was not representative of the aircraft in flight. Briefly, qualification of the actuators using real flights through field trials is a very costly and time-consuming process.[84]

## Key technologies and research challenges

During the EMA testing process, some issues and challenges are presented and need to be highlighted and solved, especially under the conditions of restrictive space and high power density. The removal of the hydraulic part introduces new constraints, such as redundancy design, reflected inertia and overload protection, and effective heat transfer for cooling the actuator. Thus, high requirements of fault tolerance, reliability, and thermal management have become main factors limiting the further development of EMAs. Here, four critical technologies and research challenges are highlighted and elaborated in the following sections.

### *Fault-tolerant motor*

The motor in safety-critical applications is designed with reliability requirement,[85] with resort to the redundancy design technique to provide a system with tolerance to failure. It includes duplicating system elements or adding backup channel. For instance, first the complete redundancy system employs two or more sets of independent actuators forming dissimilar redundancy, which includes active/active mode, active/no-load mode, and active/passive mode.[86,87] The most exemplary architecture is an EMA combined with a HSA to make a hybrid redundant actuation system. However, force fighting occurs because of the channel differences and manufacturing tolerances in the first two modes and even leads to surface fatigue. It cannot be ignored especially when it comes to an increased magnitude of position demand and load peaks.[88] The active/passive mode does not suffer the force equalization issue, but the active actuator must overcome the external force caused by the passive one at the expense of rapid response.[89,90] Second, the electrical redundancy system is backed up by two or more sets of motor and control devices as shown in Figure 11. Two independent electromechanical paths converge until there is a mechanical summing (velocity or torque) to drive mechanical transmission. In such cases, the paratactic structure that shares the rotor and dual-redundant armature windings is commonly adopted in the electric motor. However, failure isolation cannot be fulfilled in the electrical redundancy system, thus resulting in a decreased reliability.

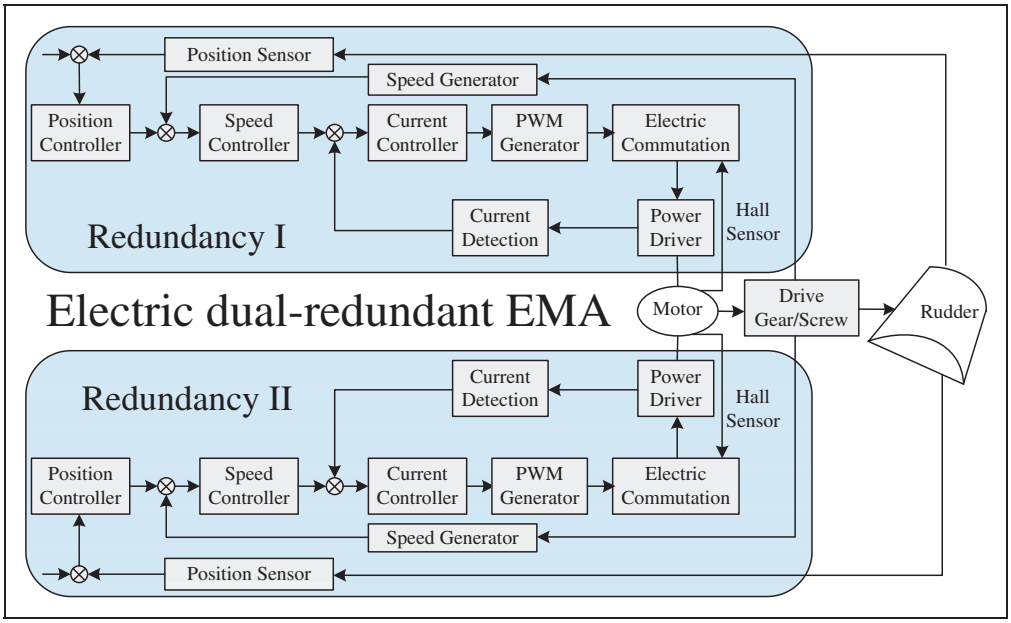


**Figure 11.** Electrical dual-redundant structure.[72]
EMA: electromechanical actuator; PWM: pulse-width modulation.

**Table 4.** Main advantages and disadvantages of three kinds of redundancy.

| | Advantages | Disadvantages |
|---|---|---|
| Complete redundancy | • Increased dissimilarity<br>• A progressive step to introduce EMAs into primary flight controls<br>• No electromagnetic coupling | • Force fighting<br>• High failure transients and dormant failures<br>• Complex control loops and reconfiguration strategy |
| Electrical redundancy | • Decreased motor size<br>• Easy to control | • No failure isolation<br>• Torque unequal because of unbalanced motor current<br>• Derating use for temperature control and load requirement[91] |
| Fault-tolerant redundancy | • Decreased volume and mass<br>• Good failure isolation<br>• High utilization level | • Complex control<br>• Uncontrolled harmonic currents even when slight magnet field distort |

EMA: electromechanical actuator.

Next-generation fault-tolerant redundancy of EMA architectures comes from electric drives with multiphase motors, which provides fault tolerance against stator coil and inverter or gate drive failures. Multiphase-based EMAs do not suffer from added rotor/load inertia associated with the redundant motor, which allows to have the same availability and reliability. The main benefits and drawbacks of the three redundancies are summarized in Table 4. Villani et al.[92,93] revealed that a sensorless five-phase permanent magnet brushless motor for aircraft flap actuation can run up to rated torque even when one or two phases were opened. Niu et al.[94] presented a multipole permanent magnet machine using fractional-slot concentrated winding and the Vernier machine structure. In this dual-structure machine, the outer and inner stator windings can either be operated simultaneously or used independently, through which the fault-tolerant capability was enhanced. Besides, the SR motor,[39] the PMSM,[95] and the fractional-slot interior permanent-magnet machine with dual three-phase windings[96] have also been validated to meet the fault tolerance requirement. However, it is generally considered undesirable in a system with more than five phases due to excessive complexity and costs, as well as the increased possibility of a single circuit failure. The reasonable range of phase number is 3, 4, or 5.[97] By providing compensation for potential failures, a fault-tolerant system can achieve reliability objectives without recourse to non-optimized redundancy or oversizing.

### High-thrust mechanical transmission

As mentioned before, motion transformation is completed by screw mechanisms such as the acme screw mechanism, BSM, and planetary roller screw mechanism (PRSM). The first two types of screw mechanisms have been used in industrial motion and load control applications for many years. Recently, EMA engineers and actuation suppliers are looking closer at the application of PRSM as a competing technology for the BSM-based EMAs. Compared with BSMs, PRSMs (Figure 12) are more suitable for those applications in which a significant shock load or large external load is applied. This is because of the incremental diameter and number of contact areas in PRSMs, which makes them a preferable technology for EMA applications. Table 5 summarizes the comparison among the three types of screw mechanisms.[98] It shows that the PRSM is the most promising mechanism for this application. However, due to the manufacturing difficulties of this structure, only a few companies have a capacity of PRSM design and manufacturing. After all, the lack of exhaustive theoretical research limits the sufficient development of PRSMs.

It is only during the past decade that literature on the exploration of PRSMs has become available. The research focuses on geometry design,[99] kinematics,[100] load distribution,[101] load-carrying capacity,[102] and efficiency.[103] Jones and Velinsky[104,105] did fundamental research on the kinematics and dynamics of the standard PRSM through analytical methods, which allows for a better understanding of the mechanism. Abevi et al.[106] built a hybrid model based on a structure of bars, beams, and non-linear springs to calculate the static load distribution and axial stiffness. Hojjat and Mahdi Agheli[107] comprehensively studied the capabilities and limitations of PRSMs and showed that large leads or extremely small leads can be realized. However, there is less work about theoretical and experimental research in multi-body contact, thermo-mechanical coupling, vibration, failure and lubrication, jamming, and diagnosis methods of PRSMs, especially when it comes to high-speed and heavy-load flight conditions. In spite of promising results on PRSM, the effort needs to increase in collection of data results and substantiations.

As EMAs are subjected to repeated cycles, the surface of mechanical components suffers degradation

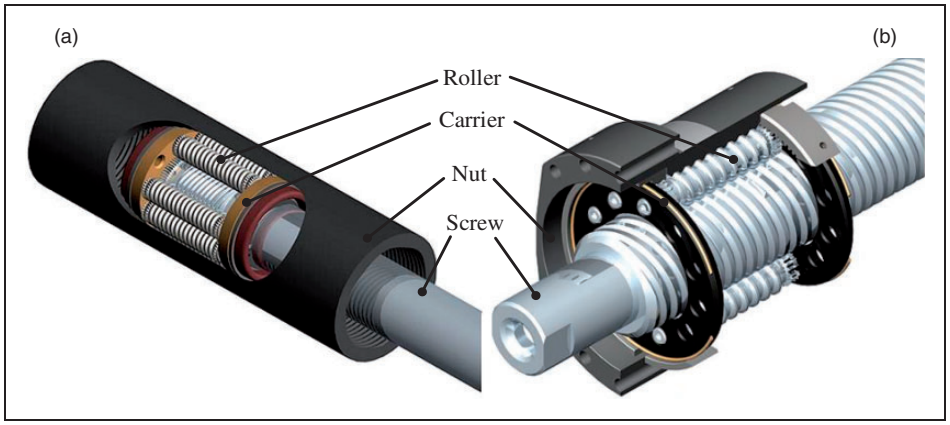


**Figure 12.** PRSM model: (a) inverted planetary roller screw mechanism and (b) standard planetary roller screw mechanism.[98]

**Table 5.** Performance comparison of screw mechanisms.[98]

| Item | Planetary roller screw | Acme screw | Ball screw |
|---|---|---|---|
| Load ratings | Very high | High | High |
| Speed | Very high | Low | Moderate |
| Acceleration | Very high | Low | Moderate |
| Lifetime | Very long, many times greater than ball screw | Very low, due to high friction and wear | Moderate |
| Stiffness | Very high | Very high | Moderate |
| Shock loads | Very high | Very high | Moderate |
| Efficiency | High | Low | Very high |
| Electronic positioning | Easy | Moderate | Easy |
| Space requirements | Minimum | Moderate | Moderate |
| Maintenance | Very low | High, due to poor wear characteristics | Moderate |

that manifests itself by a slight increase of backlash, which will affect the system stability, manoeuvrability, and flight profiles.[108] Experiments conducted by Isturiz et al.[109] showed that the backlash in screw-based EMAs can be monitored by motor currents and position sensors without the added monitoring functionality. Indeed, PRSM-incorporating gear teeth and screw mechanisms that offer numerous contacts of metallic parts are susceptible to mechanical jamming. This risk of jamming is a fatal problem for the certification of EMAs in primary flight control applications although only a few jams have been reported. On the other hand, it is worth noting for certain secondary actuations, such as the actuation of a trim horizontal stabilizer, jamming is the preferred fail mode,[32] since the load is then frozen in position.

It is commonly admitted that two types of jamming failure exist for the screw components.[110] One is catastrophic failure, where predictive maintenance is impossible and the phenomena happen without premonitions. The corresponding strategies for ensuring safe-life operation are to isolate the failure inside the actuator, such as by employing another mechanical channel (duplex actuator), by splitting the load and associating each part of it with a single actuator, or by integrating a declutching device. The other failure mode is fatigue and wear that have a developing process to a final mechanical jamming. For this kind of failure, operating parameters can be measured and predictive maintenance is viable. It occurs because the external loads fatigue the materials on the raceways under high contact stresses. Also, weak thickness of the lubricant film and low lubricant viscosity caused by temperature rise render the transmission jamming. Thus, strategy based on failure anticipation, HM is recognized efficient for increasing reliability and improving maintenance. HM system has been accomplished within the scope of the projects such as the SAFRAN/Sagem SMART WINGS project,[33] the Airbus project COVADIS,[40] and the FP7 ACTUATION2015 project.[111] It is highlighted that new integrated sensors and electronics in HM systems are also prone to failure, which increases system complexity and costs. In this way, reliability of the actuator can be affected and need to be reconsidered. The cost of HM systems, increased by adding new elements, should not be as high as to exceed maintenance cost savings.

## Multidisciplinary modelling approach

The EMA is a multidisciplinary complex concept including electromagnetic, thermal, mechanical, and control systems. The mathematical model of EMA systems is required for simulation works of control strategies and dynamic response analyses. When considering multidisciplinary modelling, it is necessary to incorporate the multi-domain coupling characteristics that may lead to inaccurate conclusions or even failure.

There are two major means for EMA system modelling. One is the typical mathematical modelling method adopted by most authors,[112–115] which is based on the system transfer function or state-space description. Nevertheless, this method allows for a less accurate description of the EMA system complexity, which limits multidisciplinary modelling. Results can be inaccurate due to some simplified assumptions of non-linearity. The other approach is to set up the multidisciplinary model using the bond graph theory and to solve for the dynamic response. This theory is based on a graphical representation idea of a physical dynamic system using arcs to represent bidirectional exchange of physical energy. Power is transmitted between components by a combination of 'effort' and 'flow'.[116] Thus, bond graphs can incorporate multiple domains and perform multidisciplinary system modelling, such as EMA and EHA systems.

*Examples of the approaches in EMA design.* As for the mathematical modelling method, most researchers design the EMAs in virtual software packages after describing the mathematical equations that govern EMA dynamic characteristics. According to the basic architecture described in 'Architecture of EMA' section, the dynamic equations of major components are listed below. The motor governing equations in the rotor reference frame ($d$–$q$ coordinates) variables can be represented as a set of differential equations

$$dI_d/dt = -RI_d/L_d + \omega_M p I_q L_q/L_d + U_d/L_d \tag{1}$$

$$dI_q/dt = -RI_q/L_q - \omega_M p I_d L_d/L_q - \omega_M p \varphi_m/L_q + U_q/L_q \tag{2}$$

$$T_{EM} = 3p/2\left[\left(L_d - L_q\right) I_d I_q + \varphi_m I_q\right] \tag{3}$$

where $I_{d,q}$, $L_{d,q}$, and $U_{d,q}$ are the current, inductance, and voltage in $q$- or $d$-axis, respectively; $R$ is the motor resistance, $\omega_M$ is the angular velocity of the motor, and $T_{EM}$ is the electromechanical torque. Thus, the equation of motion for the position $\theta_M$ of the motor is

$$J_M \ddot{\theta}_M = T_{EM} - \xi\omega_M - T_L \tag{4}$$

where $J_M$ is the motor inertia, $\xi$ is the motor damping coefficient, and $T_L$ is the motor-load torque. Using a lumped mass model, all rotating components of the gearbox, the connecting shaft to the motor as well as the rotating parts of the screw mechanism are represented by the following equation for the rotational movement

$$J_{rot}\ddot{\theta}_G = -T_L - T_{fr,rot} + T_{rot} \tag{5}$$

$$T_L = c_{rot}(\theta_G - \theta_M) + d_{rot}\left(\dot{\theta}_G - \dot{\theta}_M\right) \tag{6}$$

Here, $J_{rot}$, $c_{rot}$, and $d_{rot}$ are the lumped inertia, stiffness, and damping of those rotating components, respectively, $\theta_G$ corresponds to the angular position output of the gearbox, $T_{fr,rot}$ and $T_{rot}$ denote a Stribeck friction torque load and the load acting on the rotating parts.[113] Analogously, the translational movement of the screw mechanism is described as equations (7) and (8)

$$m_{EMA}\ddot{x}_{EMA} = -F_{sm} - F_{fr,sm} + F_{EMA} \tag{7}$$

$$F_{sm} = c_{sm}(x_{EMA} - x_{sm}) + d_{sm}(\dot{x}_{EMA} - \dot{x}_{sm}) \tag{8}$$

where $m_{EMA}$ is the mass of the translational parts, $c_{sm}$ and $d_{sm}$ are the stiffness and damping between the screw mechanism components, $x_{sm}$ and $x_{EMA}$ represent the displacement of driving part and EMA output, $F_{EMA}$ is the actuation load, $F_{sm}$ and $F_{fr,sm}$ are the acting force and friction force between the screw shaft and the nut, respectively. Finally, the transition between the rotational and translational movement is connected by the relations

$$F_{sm} = T_{rot} \cdot i_{EMA} \cdot \eta_{EMA} \tag{9}$$

$$\theta_G = x_{sm} \cdot i_{EMA} \cdot \eta_{EMA} \tag{10}$$

$$i_{EMA} = i_G \cdot 2\pi / P_h \tag{11}$$

where $i_G$ and $i_{EMA}$ stand for the gear transmission ratio and total EMA ratio, $\eta_{EMA}$ is the efficiency of the gearbox and the screw mechanism, and $P_h$ is the screw pitch. For equations (9) and (10), backlash in the kinematics of the EMA is neglected when deriving a linear model. Thus, the relationship between input motor voltage/currents to the end actuation load can be obtained when combining with proper control strategies.

For example, Habibi et al.[108] built a simulation model for a high-bandwidth EMA system with emphasis on the effect of dead zones by using multiple inner loops. Cochoy et al.[113] discussed non-linear as well as linear models for an EMA and a control surface for matching of actuator dynamics and simulation of the control laws to reduce force fighting. Arriola and Thielecke[114] created a detailed non-linear model of two parallel EMAs to enable the design of safety control functions and to reduce the reflected inertial load peaks using an active load control strategy. Chakraborty et al.[115] developed a simulation model to estimate the aerodynamic loads of primary flight control surfaces and evaluate the weight of each component.

From a load perspective, the EMAs exhibit a dominant inertial effect caused by the inertia reflected by the motor rotor through mechanical parts, compared with the single piston of the HSAs. From above equations (4), (5), (7), (9), and (10) and the kinematics of EMAs, an equivalent relation can be derived that the inertial character of actuator's rotating components ($J_M$ and $J_{rot}$) reflects on the load, which generates an effect of equivalent moving mass $m_e$

$$m_e = i_{EMA}^2 \cdot (J_M + J_{rot}) \tag{12}$$

To minimize the EMA's mass, it is expected to adopt a high reduction ratio ($i_{EMA}$). However, an adverse equivalent moving mass is also inevitably introduced, even corresponds to over 10 times[32] the equivalent translating mass of the external load. This reflected inertia increases the response time and reduces the natural frequency and can cause catastrophic shocks during the arrival to end-stop. Thus, a design methodology is needed to optimize the selection of the electrical–mechanical combination and the relationship between the actuator's mass and transmission ratios.

The bond graph theory facilitates the influence study of parameter variations, which contributes to sizing components and optimizing a heterogeneous system. Haskew and Schinstock[117] employed the modelling technique to optimize the EMA component selection for thrust vector application, based on sinusoidal steady-state analysis of an equivalent analogous circuit. Karam and Mare[61] developed an EMA lumped parameter model in a structured way, where the functional power path is highlighted by using bold bonds (Figure 13). The experiment validated the system-level EMA model based on the bond graph formalism. The methodology was also used to enable thermal balance analysis; response to jamming faults[11]; impact of compliance, friction, and clearance[118] on EMA dynamic performance. In addition, co-simulation or collaborative simulation is another effective means to design multidisciplinary systems. This method allows single sub-components to be packaged by different simulation tools that exchange information simultaneously.[119] Meanwhile, co-simulation integration requires a model interface and time constrains definition.

Recently, Budinger et al.[120] in Toulouse extensively studied on the model-based preliminary design of electromechanical systems. In order to make the best of their capability to reflect the physical constraints for sizing the actuator components, causal modelling and scaling laws are adopted in early design, which can be seen as an analysis tool for EMA components. The scaling laws, also called similarity laws, are an efficient way to investigate the effect of varying representative parameters. The scaling ratio of a given parameter is calculated as

$$l^* = \frac{l}{l'} \tag{13}$$

where $l'$ is the dimensional parameter taken as the reference and $l$ is the dimensional parameter under study. As an example, the variation of a shaft

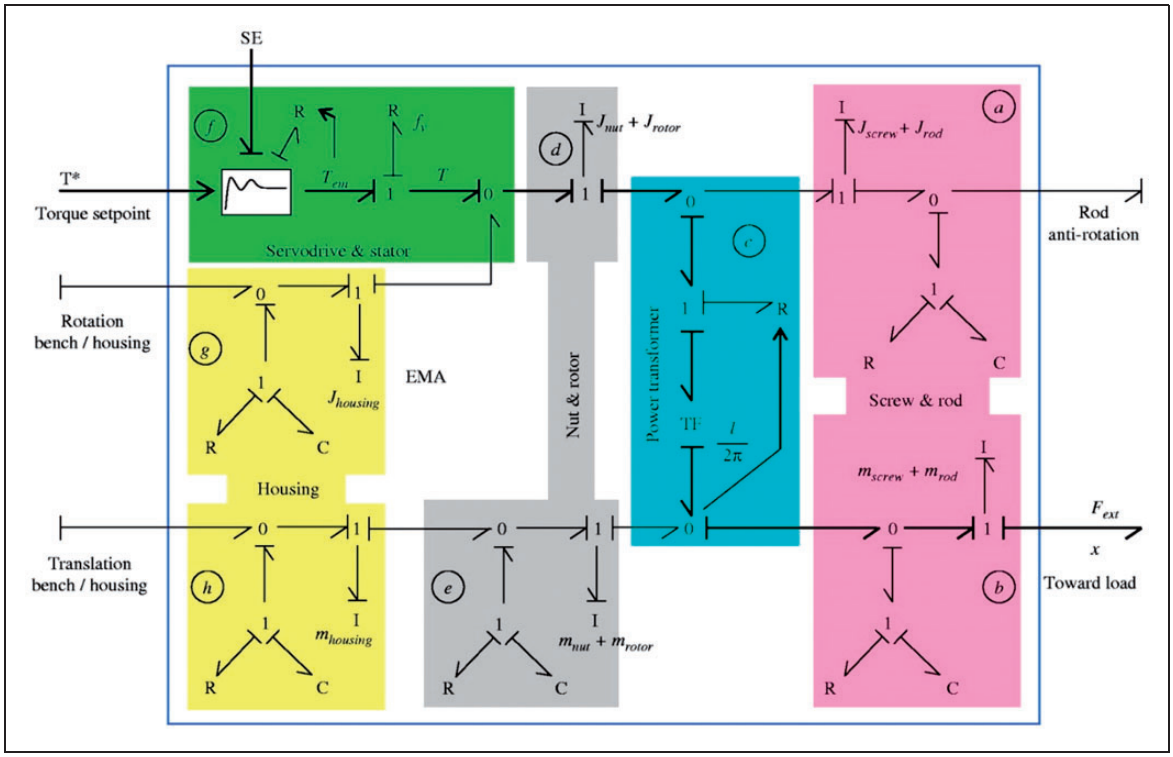


**Figure 13.** Bond graph model of the EMA. This figure was adapted from Figure 4 of Karam and Mare[61] with the permissions from the copyright owner Emerald Group Publishing Limited.
EMA: electromechanical actuator; SE: source effort.

volume in case of an identical variation for all geometrical dimensions is

$$V^* = \frac{V}{V'} = \frac{\pi r^2 l}{\pi r' 2 l'} = r^* 2 l^* \tag{14}$$

where $V$ is the volume of the shaft, $l$ is its length, and $r$ is its radius. In the same way, the evolution of the mass $M$ and rotating inertia $J$ can be calculated as a function of dimension $l$

$$M^* = l^{*3} \tag{15}$$

$$J^* = l^{*5} \tag{16}$$

Thus, the simulation parameters, integration parameters, and operational parameters of EMA components can be similarly obtained according to different definition parameters.[121,122] For example, to get an better understanding for how much the EMA might weigh when sized to some load requirements, the mass criterion that is based on geometric similarity is adopted. Table 6 is the mass comparison of bearings and ball/roller screws, gear reducers, as well as electromechanical components, such as brushless motors, and clutches. Scaling laws' use with system simulation models and inverse simulation enable quick sizing and structure evaluation even with complex mission cycles. The suitability of this methodology was validated with the preliminary sizing of the EMA for flight control surfaces and nose landing gear steering.[50] Furthermore, Chakraborty et al.[123] established a requirement-driven methodology that integrates the analysis of flight control actuation system effects and architectures to consider a vehicle and mission level of EMA's preliminary design.

## *Thermal management and thermal analysis*

An inevitable issue of the EMAs in use is heat generation and thermal management when replacing traditional hydraulic system with compact EMA system. As for the hydraulic system, the heat generated by the hydraulic actuator can be circularly brought back to the main tank where heat sources get cooled by the fluid flowing. However, heat generation can only be eliminated by local heat transfer in the EMA system. Removing of the hydraulic network means that hydraulic fluid will not be available as a convenient method of dissipating the heat.[124] As a result, it is required to facilitate temperature prediction and control in the initial design process. Currently, issues that are challenging thermal management are transient heat storage, thermal transport, and heat sinks selection. Cabin bleed air and windblown airfoils can be an approach of heat sinks.[125] Other solutions may come from technologies, such as loop heat pipes, advanced liquid cooling, heat spreaders, and phase-change materials. Advanced materials, such as nano technology, and high thermal conductivity graphite foams, were developed.[8]

Each technology accommodates particular benefits and drawbacks with regard to costs, weight, energy

**Table 6.** Established scaling laws of EMA components using mass criterion.[120]

| Component | Definition parameter | Mass | Equation number of Mass column |
|---|---|---|---|
| Rolling bearing | Dynamic load capacity $C_{nom}$ (N) | $M^* = C_{nom}^{*\,3/2}$ | (17) |
| Screw mechanism (nut) | Nominal output force $F_{n,nom}$ (N) | $M^* = F_{n,nom}^{*\,3/2}$ | (18) |
| Screw mechanism (screw) | Nominal output force $F_{s,nom}$ (N) | $M_l^* = F_{s,nom}^*$ | (19) |
| Gear reducer | Nominal output torque $T_{nom}$ (N m) | $M^* = T_{nom}^*$ | (20) |
| Brushless motor (cylindrical) | Nominal continuous torque $T_{em,nom}$ (N m) | $M^* = T_{em,nom}^{*\,3/2}$ | (21) |
| Brushless motor (annular) | Nominal continuous torque $T_{em,nom}$ (N m) | $M^* = T_{em,nom}^{*\,3/2}$ | (22) |
| Electromagnetic clutch | Torque $T$ (N m) | $M^* = T^{*3/2}$ | (23) |

EMA: electromechanical actuator.

requirement, and most importantly heat transfer performance under harsh conditions. Specifically, secondary flight control actuators work on an intermittent basis, which allows for heat dissipation within a sufficient time span. However, primary flight control surfaces are engaged throughout flight all the time, and critical attention to thermal management should be more demanding. Collection of thermal data for the validation of thermal analyses and establishing the capability for future thermal predictions is then the first driver for flight testing. Thermal parameters shall be strongly monitored in particular for EMAs on aileron applications where the surface load is high in cruise.

The main heat sources in the actuator module are the copper loss of the stator winding and the iron loss of the stator iron core in the servo motor. The heat generation depends on the stator windings current, electric power, and dimension of the motor. Therefore, motor efficiency plays a crucial role in realizing the rated thermal performance. The test conducted by Lammers[76] showed that holding presents the most significant challenge to the thermal management of EMA system. During a holding, all the electric power is converted to heat. Balaban et al.[112] described a thermal model that treats motor windings as a lumped system to determine their temperature at each step. Based on the input heat, the heat is transferred from the windings to the motor surface, and then the surface in turn loses heat to the ambient through convection and radiation. The equations that govern the thermal model are described as follows

$$\left(I^2R - \frac{T_{w,i-1} - T_s}{R_{th}}\right)dt = m_w C_{pw}\left(T_{w,i} - T_{w,i-1}\right) \tag{24}$$

$$\frac{T_{w,i-1} - T_s}{R_{th}} = hA(T_s - T_{\inf}) + \varepsilon\sigma A\left(T_s^4 - T_{\inf}^4\right) \tag{25}$$

where $I$ is winding current; $R_{th}$ is thermal resistance; $m_w$ and $C_{pw}$ are mass and specific heat of windings; $A$ is motor surface area; $T_s$, $T_w$, and $T_{\inf}$ are temperature of motor surface, winding, and ambient, respectively.

Furthermore, the heat due to friction loss that is generated by the gearbox and screw mechanism cannot be ignored because of a potential low efficiency during the transient running. Within the EMA, the heat is carried away by the flow of lubricant, which is not sunk into the actuator itself by conduction. A significant amount of heat at the frictional contact interfaces can be naturally generated in a compact and high-load mechanical system. The conductive heat leads to the temperature rise of transmission components that subsequently results in thermal drift and error as well as the actuation accuracy degradation. Therefore, thermal analysis must be implemented for a complete flight cycle including high-power motors and frictional components. The temperature field modelling of the servo motor and the EMA module is usually completed by the finite element method (FEM) and the equivalent thermal network method.

The FEM is the most effective method in analysing and predicting the heat generation and conduction, including non-linear electromagnetics, coupled thermomechanical, and heat transfer to simulate the complete object. The thermal network analysis provides a rapid tool for predicting thermal distribution without increasing drastically the complexity of the model implementation. For example, Woodburn et al.[126] described a lumped-element model of the permanent magnet motor in the EMA system. The parameters, such as non-linear inductance, thermal resistances,

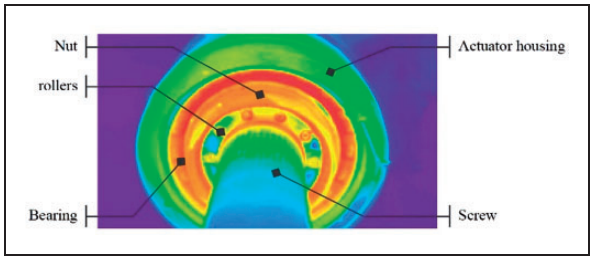


**Figure 14.** Thermography image of an EMA. This figure was adapted from Figure 6.27 of Mare[32] with the permissions from the copyright owner John Wiley and Sons.

and capacitances, were adjusted using FE models. In order to evaluate the thermal distribution and error of the PRSM, a thermomechanical model based on FEM was developed by Ma et al.[127] Pasies et al.[128] demonstrated a novel technique using an electrothermal bus co-simulation to integrate multi-physics models. Moreover, temperature tests of EMA components are the most reliable method, but it is relatively time consuming and vulnerable to the external condition. Figure 14 illustrates the thermography image (temperatures vary from 20 to 120 °C) at the rod of an EMA,[129] after a full sinus load of 30 min. For the time being, there are limited interior temperature experiments and system-level thermal analysis available to meet EMA system thermal design requirements. The thermal research also contributes to predicting the remaining useful life of EMAs based on temperature restrictions.[130]

## Conclusions

As the MEA/AEA becomes popular in aerospace applications, the EMA is developed as the next generation of actuation system involving flight controls, landing gears, engines, and TVCs. It has been tested and validated successfully in several large-scale research projects mentioned in this review. Due to the increased safety and reliability, easier and reduced maintenance compared to the traditional hydraulic system, EMA system is being extensively applied in commercial and military aircraft fields. From the presented key technologies and research challenges in fight control application, several comments on EMA system development are given: (1) The EMA is moving towards a highly integrated system by means of some critical technologies such as multidisciplinary optimization, integrated design, and direct-drive architecture manufacture. (2) The EMA is developed towards high reliability and high power density. The fault-tolerant servo motor, the advanced mechanical transmission mechanism, and the redundant system topologies such as hybrid actuator configurations are usually adopted to comply with the trend. (3) The future EMA research will be directed to jamming-free systems and condition monitoring testing systems, which have a better diagnostic ability along with health management techniques in its early stage and predicting the remaining life of the faulty components. The HM function is identified as an important driver for the EMA technology used in the future aircraft architecture.

The EMA is a relatively new actuation concept for the MEA/AEA and has a high potential of improvement. Although the extensive verification and testing implemented in past several decades, EMAs are not mature enough to replace traditional HSAs in normal mode for safety-critical surfaces. A practical approach can be adopted with the best combination of hydraulic and electric in such flight control applications. This weakness would be overcome owing to the attempts of modularization, standardization, and increased requirement of EMAs.

### Declaration of Conflicting Interests

The author(s) declared no potential conflicts of interest with respect to the research, authorship, and/or publication of this article.

### Funding

The author(s) disclosed receipt of the following financial support for the research, authorship, and/or publication of this article: This research work is supported by the National Natural Science Foundation of China (Grant No. 51505381, 51275423), 111 Project of China (Grant No. B13044), the Fundamental Research Funds for the Central Universities (3102014ZD0035), China Postdoctoral Science Foundation funded project (2014M552483), and China Scholarship Council (CSC).

### References

1. Janker P, Claeyssen F, Grohmann B, et al. New actuators for aircraft and space applications. In: *Eleventh international conference on new actuators*, Bremen, Germany, 9–11 June 2008, pp.346–354.
2. Rosero JA, Ortega JA, Aldabas E, et al. Moving towards a more electric aircraft. *IEEE Aero El Syst Mag* 2007; 22: 3–9.
3. Garcia A, Cusido I, Rosero JA, et al. Reliable electromechanical actuators in aircraft. *IEEE Aero El Syst Mag* 2008; 23: 19–25.
4. AbdElhafez A and Forsyth A. A review of more-electric aircraft. In: *Thirteenth international conference on aerospace science & aviation technology (ASAT-13)*, 26–28 May 2009, paper no. ASAT-13-EP-01. Piscataway, NJ, USA: IEEE.
5. Botten SL, Whitley CR and King AD. Flight control actuation technology for next-generation all-electric aircraft. *Technol Rev J* 2000; 23: 55–68.
6. Liscouët J, Maré JC and Budinger M. An integrated methodology for the preliminary design of highly reliable electromechanical actuators: search for architecture solutions. *Aerosp Sci Technol* 2012; 22: 9–18.
7. Chakraborty I, Mavris DN, Emeneth M, et al. An integrated approach to vehicle and subsystem sizing and analysis for novel subsystem architectures. *Proc IMechE, Part G: J Aerospace Engineering* 2015; 230: 496–514.

8. Blanding D. Subsystem design and integration for the more electric aircraft. In: *5th international energy conversion engineering conference and exhibit (IECEC)*, St. Louis, Missouri, 2007, pp.31–38. Reston, VA, USA: American Institute of Aeronautics and Astronautics.
9. Croke S and Herrenschmidt J. More electric initiative-power-by-wire actuation alternatives. In: *Aerospace and electronics conference, proceedings of the IEEE 1994 National*, Dayton, OH, USA, 23–27 May 1994, pp.1338–1346. Piscataway, NJ, USA: IEEE.
10. Nelson T. 787 systems and performance, http://myhres.com/Boeing-787-Systems-and-Performance.pdf (2005, accessed).
11. Fu J, Mare JC and Fu YL. Modelling and simulation of flight control electromechanical actuators with special focus on model architecting, multidisciplinary effects and power flows. *Chin J Aeronaut* 2017; 30: 47–65.
12. Sitz JR. F-18 systems research aircraft facility. In: *1992 aerotech conference*, Anaheim, CA, USA, 5–8 October 1992, pp.1–27. Anaheim, CA, USA: National Aeronautics and Space Administration.
13. Williams K and Brown D. Milestone achieved for all-electric airplane technology, www.nasa.gov/home/hqnews/1997/97-274.txt (1997, accessed 20 November).
14. Navarro R. *Performance of an electro-hydrostatic actuator on the F-18 systems research aircraft*. Report for NASA. Report no. TM-97-206224, October 1997. Anaheim, CA, USA: National Aeronautics and Space Administration.
15. Charrier JJ and Kulshreshtha A. Electric actuation for flight and engine control; evolution and current trend. In: *Forty-fifth AIAA aerospace sciences meeting and exhibit*, Reno, Nevada, 8–11 January 2007, pp.1–20. Reston, VA, USA: American Institute of Aeronautics and Astronautics.
16. Wang ZL, Qiu LH and Li J. Actuation systems used for power-by-wire, www.paper.edu.cn/releasepaper/content/200408-25 (2004, accessed).
17. Sarlioglu B and Morris CT. More electric aircraft: review, challenges, and opportunities for commercial transport aircraft. *IEEE Trans Transp Electrification* 2015; 1: 54–64.
18. Van den Bossche D. The evolution of the airbus flight control actuation systems. In: *Proceedings of the 3rd international fluid power conference*, Aachen, Germany, 2002.
19. Chakraborty I, Trawick DR, Jackson D, et al. Electric control surface actuator design optimization and allocation for the more electric aircraft. In: *2013 aviation technology, integration, and operations conference*, Los Angeles, CA, 12–14 August 2013, pp.1–17. Reston, VA, USA: American Institute of Aeronautics and Astronautics.
20. Antonelli MG, Bucci G, Ciancetta F, et al. Automatic test equipment for avionics Electro-Mechanical Actuators (EMAs). *Measurement* 2014; 57: 71–84.
21. Todeschi M and Baxerres L. Health monitoring for the flight control EMAs. *IFAC-PapersOnLine* 2015; 48: 186–193.
22. Wagner H, Nikolov G, Bierig A, et al. Challenges for health monitoring of electromechanical flight control actuation systems. SAE paper 2011-01-2701, 2011.
23. Tutt GE and Jansen JA. Dynamics of the Apollo electromechanical actuator. *J Space Rockets* 1968; 5: 541–546.
24. Edge JT. An electromechanical actuator technology development program. SAE paper 780581, 1978.
25. Albright J and Moore L. Development and implementation of electromechanical actuators for the X-38 atmospheric test vehicles. In: *AIAA atmospheric flight mechanics conference and exhibit*, Honolulu, Hawaii, 18–21 August 2008, pp.1–38. Reston, VA, USA: American Institute of Aeronautics and Astronautics.
26. Di Rito G, Galatolo R and Schettini F. Self-monitoring electro-mechanical actuator for medium altitude long endurance unmanned aerial vehicle flight controls. *Adv Mech Eng* 2016; 8: 1–11.
27. Mare JC. General considerations. In: JP Bourrieres (ed.) *Aerospace actuators 1: needs, reliability and hydraulic power solutions*. London: ISTE Ltd, 2016, pp.1–32.
28. Rubertus DP, Hunter LD and Cecere GJ. Electromechanical actuation technology for the all-electric aircraft. *IEEE T Aero El Syst* 1984; AES-20: 243–249.
29. Norton WJ. *Advanced electromechanical actuation system (EMAS) flight test*. Report for 4950th Test Wing. Report no. AD-A176-148b, June 1986. Washington: AFWAL.
30. Jensen SC, Jenney GD and Dawson D. Flight test experience with an electromechanical actuator on the F-18 systems research aircraft. In: *Nineteenth digital avionics systems conference*, 2000, pp.2E3/1-2E310.
31. Jomier T. *More open electrical technologies*. Report for AF-DEL-MOET Consortium Partners. Report no. 0001-09-R1, 2009.
32. Mare JC. Electro-mechanical actuators. In: JP Bourrieres (ed.) *Aerospace actuators 2: signal-by-wire and power-by-wire*. London: ISTE Ltd, 2016, pp.1–32.
33. Derrien JC and Sécurité SD. Electromechanical actuator (EMA) advanced technologies for flight controls. In: *28th international congress of the aeronautical sciences*, Brisbane, Australia, 23–28 September 2012, pp.1–10. Bonn, Germany: International Council of the Aeronautical Sciences.
34. Van der Linden FL, Schlegel C, Christmann M, et al. Implementation of a modelica library for simulation of electromechanical actuators for aircraft and helicopters. In: *Proceedings of the 10th international modelica conference*, Lund, Sweden, 10–12 March 2014, pp.757–766. Linköping, Sweden: LiU Electronic Press.
35. Gilmour E. Requirements definition and qualification for a HEAT fly-by-wire system. In: *Thirtieth European rotorcraft forum*, Marseille, France, 14–16 September 2004, pp.1–11. France: European Rotorcraft Forum.
36. Rottach M, Gerada C and Wheeler P. Helicopter EMA system: electrical drive optimization and test. In: *Proceedings of the 6th international conference on recent advances in aerospace actuation systems and components*, Toulouse, France, 2–3 April 2014, pp.9–13. Toulouse, France: R3ASC.
37. Gianfranceschi M, Jacazio G and Wang J. High bandwidth electromechanical actuator for swashplateless blade control system. In: *Proceedings of the 6th international conference on recent advances in aerospace actuation systems and components*, Toulouse, France, 2–3 April 2014, pp.1–8. Toulouse, France: R3ASC.

38. Bennett JW. *Fault tolerant electromechanical actuators for aircraft*. PhD Thesis, Newcastle University, UK, 2010.
39. Fronista GL and Bradbury G. An electromechanical actuator for a transport aircraft spoiler surface. In: *IECEC-97 proceedings of the thirty-second intersociety energy conversion engineering conference*, Honolulu, HI, USA, 27 July–1 August 1997, pp.694–698. Piscataway, NJ, USA: IEEE.
40. Todeschi M and Baxerres L. Airbus-health monitoring for the flight control EMAs: 2014 status and perspectives. In: *Proceedings of the 6th international conference on recent advances in aerospace actuation systems and components*, Toulouse, France, 2–3 April 2014, pp.73–83. Toulouse, France: R3ASC.
41. Mare JC. Combining hydraulics and electrics for innovation and performance improvement in aerospace actuation. In: *Proceedings of the 12th Scandinavian international conference on fluid power*, Tampere, Finland, 18–20 May 2011, pp.255–270.
42. Chevalier PY, Grac S and Liegeois PY. More electrical landing gear actuation systems. In: *Proceedings of the 4th international conference on recent advances in aerospace actuation systems and components*, Toulouse, France, 5–7 May 2010, pp.9–16. Toulouse, France: R3ASC.
43. Iordanidis G, Bagnall L, Morris J, et al. An overview of modelling and simulation activities for an all-electric nose wheel electric system. In: *Proceedings of the 4th international conference on recent advances in aerospace actuation systems and components*, Toulouse, France, 5–7 May 2010, pp.137–144. Toulouse, France: R3ASC.
44. Chico P. Electric brake. In: *Proceedings of the 6th international conference on recent advances in aerospace actuation systems and components*, Toulouse, France, 2–3 April 2014, pp.25–28. Toulouse, France: R3ASC.
45. Mare JC and Fu J. Review on signal-by-wire and power-by-wire actuation for more electric aircraft. *Chin J Aeronaut* 2017; 30: 857–870.
46. Lemor PC. The roller screw, an efficient and reliable mechanical component of electro-mechanical actuators. In: *Proceedings of the 31st intersociety energy conversion engineering conference*, Washington, DC, USA, 11–16 August 1996, pp.215–220. Piscataway, NJ, USA: IEEE.
47. Alle N, Hiremath SS, Makaram S, et al. Review on electro hydrostatic actuator for flight control. *Int J Fluid Power* 2016; 17: 125–145.
48. Torabzadeh-Tari M. *Dimensioning tools of MEA actuator systems, including modeling, analysis and technology comparison*. PhD Dissertation, KTH Electrical Engineering, Sweden, 2008.
49. Liscouët J, Mare J and Orieux S. Automated generation, selection and evaluation of architectures for electromechanical actuators. In: *Twenty-sixth international conference of the aeronautical sciences*, Anchorage, Alaska, USA, 14–19 September 2008, pp.14–19. Bonn, Germany: International Council of the Aeronautical Sciences.
50. Budinger M, Liscouët J, Orieux S, et al. Automated preliminary sizing of electromechanical actuator architectures. In: *ELECTRIMACS 2008 conference*, Québec, Canada, June 2008.
51. Budinger M, Reysset A, Halabi TE, et al. Optimal preliminary design of electromechanical actuators. *Proc IMechE, Part G: J Aerospace Engineering* 2013; 228: 1598–1616.
52. Budinger M. Preliminary design and sizing of actuation systems, https://hal.archives-ouvertes.fr/tel-01112448/file/HDR_Budinger_global_final_72dpi.pdf, UPS Toulouse (2014, accessed 3 February 2015).
53. Torabzadeh-Tari M. *Analysis of electro-meachanical actuator systems in more electric aircraft applications*. PhD Dissertation, Royal Institute of Technology, Sweden, 2005.
54. Bennett JW, Mecrow BC, Atkinson DJ, et al. Safety-critical design of electromechanical actuation systems in commercial aircraft. *IET Electr Power Appl* 2011; 5: 37–47.
55. Wachendorf N, Thielecke F, Carl U, et al. Multivariable controller design for a trimmable horizontal stabilizer actuator with two primary load paths. In: *26th international congress of the aeronautical sciences*, Anchorage, Alaska, USA, 14–19 September 2008, pp.1–12. Bonn, Germany: International Council of the Aeronautical Sciences.
56. Gerada C, Bradley K, Whitley C, et al. Integrated machine design for electro-mechanical actuation. In: *2007 IEEE international symposium on industrial electronics*, Vigo, Spain, 4–7 June 2007, pp.1305–1310. Piscataway, NJ, USA: IEEE.
57. Fu YL, Zhou WX, Zhang Y, et al. Robust and perfect tracking control for direct drive EMA system. In: *Intelligent control and information processing (ICICIP)*, Dalian, China, 13–15 August 2010, pp.738–743. Piscataway, NJ, USA: Institute of Electrical and Electronics Engineers.
58. Hong G and Wei X. Development of electromechanical actuators. *Acta Aeronaut Astronaut Sin* 2007; 28: 620–627.
59. Schinstock DE and Haskew TA. Dynamic load testing of roller screw EMAs. In: *Proceedings of the 31st intersociety energy conversion engineering conference*, Washington, DC, USA, 11–16 August 1996, pp.221–226. Piscataway, NJ, USA: IEEE.
60. Mare JC. Dynamic loading systems for ground testing of high speed aerospace actuators. *Aircr Eng Aerosp Technol* 2006; 78: 275–282.
61. Karam W and Mare JC. Modelling and simulation of mechanical transmission in roller-screw electromechanical actuators. *Aircr Eng Aerosp Technol* 2009; 81: 288–298.
62. Smith MJ, Byington CS, Watson MJ, et al. Experimental and analytical development of health management for electro-mechanical actuators. In: *2009 IEEE aerospace conference*, Big Sky, MT, USA, 7–14 March 2009, pp.1–14. Piscataway, NJ, USA: IEEE.
63. Schroeder JB and Chen R. An overview of electrically powered control actuation health management. SAE paper 2010-01-1746, 2010.
64. Karam W. *Investigation into the electromechanical actuator when used for high performance force control*. PhD Dissertation, INSA Toulouse, France, 2007.
65. Koopmans MT, Mattheis C and Lawrence A. *Electromechanical actuator test stand for in-flight experiments*. Bachelor Dissertation, Mechanical Engineering Department, California Polytechnic State University, USA, 2009.
66. Ismail MA, Balaban E and Spangenberg H. Fault detection and classification for flight control

electromechanical actuators. In: *2016 IEEE aerospace conference*, Big Sky, MT, USA, 5–12 March 2016, pp.1–10. Piscataway, NJ, USA: IEEE.
67. Zhang Y, Liu D, Yu J, et al. EMA remaining useful life prediction with weighted bagging GPR algorithm. *Microelectron Reliab* 2017; 75: 253–263.
68. Tursini M, Fabri G, Loggia ED, et al. Parallel positioning of twin EMAs for fault-tolerant flap applications. In: *2012 electrical systems for aircraft, railway and ship propulsion*, Bologna, Italy, 16–18 October 2012, pp.1–6. Piscataway, NJ, USA: Institute of Electrical and Electronics Engineers.
69. Castellini L, Andrea MD and Borgarelli N. Analysis and design of a linear electro-mechanical actuator for a high lift system. In: *2014 international symposium on power electronics, electrical drives, automation and motion*, Ischia, Italy, 18–20 June 2014, pp.243–247. Piscataway, NJ, USA: IEEE.
70. Legrand B, Loyer J, Manon G, et al. EMA technology development. In: *MOET project consortium*, 2009.
71. Layton DS and Gaines VG. F-22 actuator dynamic stiffness (impedance) testing. In: *Forty-eighth AIAA/ASME/ASCE/AHS/ASC structures, structural dynamics, and materials conference*, Honolulu, Hawaii, 2007. American Institute of Aeronautics and Astronautics.
72. Kulshreshtha A and Charrier J. Electric actuation for flight and engine control: evolution and challenges. In: *SAE-ACGSC meeting*, 2007.
73. Spangenberg H and Vechtel D. Failure detection, identification and reconfiguration: applications for a modular iron bird. In: *AIAA modeling and simulation technologies conference and exhibit*, Hilton Head, South Carolina, 20–23 August 2007, pp.1–8. Reston, VA, USA: American Institute of Aeronautics and Astronautics.
74. Trentin A, Zanchetta P, Wheeler P, et al. Performance evaluation of two stage matrix converters for EMA in aircraft applications. In: *2009 IEEE energy conversion congress and exposition*, San Jose, CA, USA, 20–24 September 2009, pp.1199–1204. Piscataway, NJ, USA: IEEE.
75. Barnett S. *Laboratory test set-up to evaluate electromechanical actuation system for aircraft flight control*. Master Dissertation, University of Dayton, USA, 2015.
76. Lammers ZA. *Thermal management of electromechanical actuation system for aircraft primary flight control surfaces*. Master Dissertation, University of Dayton, USA, 2014.
77. Racine E, Lammers Z, Barnett S, et al. Energy analysis of electromechanical actuator under simulated aircraft primary flight control surface load. SAE paper 2014-01-2182, 2014.
78. Isturiz A, Mugarra A and Vinals J. Electromechanical actuators for aero-engines to control IGVs. In: *Proceedings of the 6th international conference on recent advances in aerospace actuation systems and components*, Toulouse, France, 2–3 April 2014, pp.14–18. Toulouse, France: R3ASC.
79. Kudlac MT, Weaver HF and Cmar MD. Thermal vacuum integrated system test at B-2. *Cryogenics* 2012; 52: 296–300.
80. Barnett SA, Lammers Z, Razidlo B, et al. Test set-up for electromechanical actuation systems for aircraft flight control. SAE paper 2012-01-2203, 2012.
81. Todeschi M. Airbus-EMAs for flight controls actuation system-an important step achieved in 2011. SAE paper 2011-01-2732, 2011.
82. Balaban E, Saxena A, Narasimhan S, et al. Prognostic health-management system development for electromechanical actuators. *J Aerosp Inform Syst* 2015; 12: 329–344.
83. Van Den Bossche D. The A380 flight control electrohydrostatic actuators, achievements and lessons learnt. In: *25th international congress of the aeronautical sciences*, Hamburg, Germany, 3–8 September 2006, pp.1–8. Bonn, Germany: International Council of the Aeronautical Sciences.
84. Ullah N. Loads simulator system for testing and qualification of flight actuators. In: Agarwal RK (ed) *Recent progress in some aircraft technologies*. Rijeka: InTech, 2006, pp.77–87.
85. El-Refaie AM. Fault-tolerant permanent magnet machines: a review. *IET Electr Power Appl* 2011; 5: 59–74.
86. Wang LJ, Mare JC and Fu YL. Investigation in the dynamic force equalization of dissimilar redundant actuation systems operating in active active mode. In: *28th international congress of the aeronautical sciences*, Brisbane, Australia, 23–28 September 2012, pp.1–8. Bonn, Germany: International Council of the Aeronautical Sciences.
87. Fan DL, Fu YL, Guo YQ, et al. Dynamic force equalization for dissimilar redundant actuator system. *J Beijing Univ Aeronaut Astronaut* 2015; 41: 234–240.
88. Wang LJ and Mare JC. A force equalization controller for active/active redundant actuation system involving servo-hydraulic and electro-mechanical technologies. *Proc IMechE, Part G: J Aerospace Engineering* 2013; 228: 1768–1787.
89. Fu YL, Qi HT, Wang LJ, et al. Research on operating modes in hybrid actuation systems. *Acta Aeronaut Astronaut Sin* 2010; 31: 1177–1184.
90. Cochoy O, Carl UB and Thielecke F. Integration and control of electromechanical and electrohydraulic actuators in a hybrid primary flight control architecture. In: *Proceedings of the 3rd international conference on recent advances in aerospace actuation systems and components*, Toulouse, France, 13–15 June 2007, pp.1–8. Toulouse, France: R3ASC.
91. Hao Z, Hu Y and Huang W. Development of fault-tolerant permanent magnet machine and its control system in electro-mechanical actuator. *Acta Aeronaut Astronaut Sin* 2008; 29: 149–158.
92. Villani M, Tursini M, Fabri G, et al. High reliability permanent magnet brushless motor drive for aircraft application. *IEEE T Ind Electron* 2012; 59: 2073–2081.
93. Tursini M, Fabri G, Loggia ED, et al. Parallel positioning of twin EMAs for fault-tolerant flap applications. In: *2012 electrical systems for aircraft, railway and ship propulsion*, Bologna, Italy, 16–18 October 2012, pp.1–6. Reston, VA, USA: Institute of Electrical and Electronics Engineers.
94. Niu S, Ho SL and Fu WN. A novel direct-drive dual-structure permanent magnet machine. *IEEE T Magn* 2010; 46: 2036–2039.
95. Guo H, Xu JQ and Kuang XL. A novel fault tolerant permanent magnet synchronous motor with improved optimal torque control for aerospace application. *Chin J Aeronaut* 2015; 28: 535–544.

96. Barcaro M, Bianchi N and Magnussen F. Faulty operations of a PM fractional-slot machine with a dual three-phase winding. *IEEE T Ind Electron* 2011; 58: 3825–3832.
97. Cao W, Mecrow BC, Atkinson GJ, et al. Overview of electric motor technologies used for more electric aircraft (MEA). *IEEE T Ind Electron* 2012; 59: 3523–3531.
98. Shelton G. Roller screw actuators: benefits, selection and maintenance, http://exlar.com/pdf/?pdf=/content/uploads/2014/09/Roller-Screw-Actuators.pdf (2010, accessed).
99. Jones MH and Velinsky SA. Contact kinematics in the roller screw mechanism. *J Mech Des* 2013; 135: 051003–051003-10.
100. Liu YQ, Wang JS, Cheng HX, et al. Kinematics analysis of the roller screw based on the accuracy of meshing point calculation. *Math Probl Eng* 2015; 2015: 303972–303972-10.
101. Zhang WJ, Liu G, Tong RT, et al. Load distribution of planetary roller screw mechanism and its improvement approach. *Proc IMechE, Part C: J Mechanical Engineering Science* 2015; 230: 3304–3318.
102. Jones MH and Velinsky SA. Stiffness of the roller screw mechanism by the direct method. *Mech Based Des Struct* 2013; 42: 17–34.
103. Velinsky SA, Chu B and Lasky TA. Kinematics and efficiency analysis of the planetary roller screw mechanism. *J Mech Des* 2009; 131: 011016–011016-8.
104. Jones MH and Velinsky SA. Kinematics of roller migration in the planetary roller screw mechanism. *J Mech Des* 2012; 134: 061006–061006-6.
105. Jones MH, Velinsky SA and Lasky TA. Dynamics of the planetary roller screw mechanism. *J Mech Robot* 2015; 8: 014503–014503-6.
106. Abevi F, Daidie A, Chaussumier M, et al. Static load distribution and axial stiffness in a planetary roller screw mechanism. *J Mech Des* 2015; 138: 012301–012301-11.
107. Hojjat Y and Mahdi Agheli M. A comprehensive study on capabilities and limitations of roller-screw with emphasis on slip tendency. *Mech Mach Theory* 2009; 44: 1887–1899.
108. Habibi S, Roach J and Luecke G. Inner-loop control for electromechanical (EMA) flight surface actuation systems. *J Dyn Syst-T ASME* 2008; 130: 051002–051002-13.
109. Isturiz A, Vinals J, Abete JM, et al. Health monitoring strategy for electromechanical actuator systems and components. Screw backlash and fatigue estimation. In: *Proceedings of the 5th international conference on recent advances in aerospace actuation systems and components*, Toulouse, France, 13–14 June 2012, pp.30–38. Toulouse, France: R3ASC.
110. Hebrard Y and Magnin C. EMA key components and associated monitoring. In: *Proceedings of the 5th international conference on recent advances in aerospace actuation systems and components*, Toulouse, France, 13–14 June 2012, pp.129–137. Toulouse, France: R3ASC.
111. Van der Linden FL, Dreyer N and Dorkel A. EMA health monitoring: an overview. In: *Proceedings of the 5th international conference on recent advances in aerospace actuation systems and components*, Toulouse, France, 16–17 March 2016, pp.21–26. Toulouse, France: R3ASC.
112. Balaban E, Saxena A, Goebel K, et al. Experimental data collection and modeling for nominal and fault conditions on electro-mechanical actuators. In: *Annual conference of the prognostics and health management society*, San Diego, CA, USA, 27 September–1 October 2009, pp.1–15. Piscataway, NJ, USA: IEEE.
113. Cochoy O, Hanke S and Carl UB. Concepts for position and load control for hybrid actuation in primary flight controls. *Aerosp Sci Technol* 2007; 11: 194–201.
114. Arriola D and Thielecke F. Design of fault-tolerant control functions for a primary flight control system with electromechanical actuators. In: *2015 IEEE AUTOTESTCON*, National Harbor, MD, USA, 2–5 November 2015, pp.393–402. Piscataway, NJ, USA: IEEE.
115. Chakraborty I, Jackson D, Trawick DR, et al. Development of a sizing and analysis tool for electro-hydrostatic and electromechanical actuators for the more electric aircraft. In: *2013 aviation technology, integration, and operations conference*, Los Angeles, CA, 12–14 August 2013. Reston, VA, USA: American Institute of Aeronautics and Astronautics.
116. Karnopp DC, Margolis DL and Rosenberg RC. *System dynamics: modeling, simulation, and control of mechatronic systems*. Hoboken, NJ, USA: John Wiley & Sons, 2012.
117. Haskew TA and Schinstock DE. Optimal design of electromechanical actuators for active loads. *IEEE/ASME Trans Mech* 1998; 3: 129–137.
118. Qiao G, Liu G, Ma SJ, et al. Dynamic characteristic analysis of electro-mechanical actuator based on planetary roller screw mechanism. *J Vib Shock* 2016; 35: 82–88.
119. Debiane A, Daclat J, Denis R, et al. PRESAGE: virtual testing platform application to thrust reverser actuation system. In: *Third international conference on systems and control*, Algiers, Algeria, 29–31 October 2013, pp.1127–1133. Piscataway, NJ, USA: IEEE.
120. Budinger M, Liscouët J, Hospital F, et al. Estimation models for the preliminary design of electromechanical actuators. *Proc IMechE, Part G: J Aerospace Engineering* 2011; 226: 243–259.
121. Fraj A, Budinger M, El Halabi T, et al. Modelling approaches for the simulation-based preliminary design and optimization of electromechanical and hydraulic actuation systems. In: *Fifty-third AIAA/ASME/ASCE/AHS/ASC structures, structural dynamics and materials conference*, Honolulu, Hawaii, 23–26 April 2012. Reston, VA, USA: American Institute of Aeronautics and Astronautics.
122. Liscouët J, Budinger M, Mare JC, et al. Modelling approach for the simulation-based preliminary design of power transmissions. *Mech Mach Theory* 2011; 46: 276–289.
123. Chakraborty I, Mavris DN, Emeneth M, et al. An integrated approach to vehicle and subsystem sizing and analysis for novel subsystem architectures. *Proc IMechE, Part G: J Aerospace Engineering* 2015; 230: 496–514.

124. Lawson CP and Pointon JM. Thermal management of electromechanical actuation on an all-electric aircraft. In: *26th international congress of the aeronautical sciences*, Anchorage, Alaska, USA, 14–19 September 2008, pp.1–11. Bonn, Germany: International Council of the Aeronautical Sciences.
125. Woodburn D, Wu T, Chow L, et al. Dynamic heat generation modeling of high performance electromechanical actuator. In: *Forty-eighth AIAA aerospace sciences meeting including the new horizons forum and aerospace exposition*, Orlando, Florida, 4–7 January 2010. Reston, VA, USA: American Institute of Aeronautics and Astronautics.
126. Woodburn D, Wu T, Zhou L, et al. High-performance electromechanical actuator dynamic heat generation modeling. *IEEE T Aero El Syst* 2014; 50: 530–541.
127. Ma SJ, Liu G, Qiao G, et al. Thermo-mechanical model and thermal analysis of hollow cylinder planetary roller screw mechanism. *Mech Based Des Struct* 2015; 43: 359–381.
128. Pasies-Rubert O, Mur C, Garay M, et al. Benefits of multiphysics models integration through cosimulation-case study: heat monitoring on a primary flight control EMA. In: *Proceedings of the 6th international conference on recent advances in aerospace actuation systems and components*, Toulouse, France, 2–3 April 2014, pp.144–149. Toulouse, France: R3ASC.
129. Grand S and Valemboid JM. Electromechanical actuators design for thrust vector control. In: *Proceedings of the 2nd international conference on recent advances in aerospace actuation systems and components*, Toulouse, France, 24–26 November 2004, pp.21–27. Toulouse, France: R3ASC.
130. Zhang Y, Peng X, Peng Y, et al. Weighted bagging gaussion process regression to predict remaining useful life of electro-mechanical actuator. In: *2016 prognostics and system health management conference*, Chengdu, China, 19–21 October 2016, pp.1–6. Piscataway, NJ, USA: Institute of Electrical and Electronics Engineers.

## Appendix

### Notation

| | |
|---|---|
| $A$ | motor surface area |
| $c_{rot}$ | lumped stiffness of rotating components |
| $c_{sm}$ | stiffness between the screw mechanism components |
| $C_{pw}$ | specific heat of windings |
| $d$ | rotor reference frame variable |
| $d_{rot}$ | lumped damping of rotating components |
| $d_{sm}$ | damping between the screw mechanism components |
| $F_{fr,sm}$ | friction force between screw shaft and nut |
| $F_{sm}$ | acting force between screw shaft and nut |
| $F_{EMA}$ | actuation load |
| $h$ | heat transfer coefficient |
| $i$ | time step |
| $i_{EMA}$ | EMA ratio |
| $i_G$ | gear transmission ratio |
| $I$ | current |
| $J^*$ | scaling ratio of rotating inertia |
| $J_M$ | motor inertia |
| $J_{rot}$ | lumped inertia of rotating components |
| $l$, $l'$, $l^*$ | dimensional parameter, referenced dimensional parameter, scaling ratio of dimensional parameter |
| $L$ | inductance |
| $m_e$ | equivalent moving mass |
| $m_w$ | mass of windings |
| $m_{EMA}$ | mass of the translational parts |
| $M^*$ | scaling ratio of mass |
| $M_l^*$ | scaling ratio of mass per unit length |
| $p$ | number of pole pairs |
| $P_h$ | screw pitch |
| $q$ | rotor reference frame variable |
| $r$, $r'$, $r^*$ | radius, referenced radius, scaling ratio of radius |
| $R$ | motor resistance |
| $R_{th}$ | thermal resistance |
| $t$ | time |
| $T_{fr,rot}$ | Stribeck friction torque load |
| $T_{\inf}$ | temperature of ambient |
| $T_{rot}$ | load acting on the rotating parts |
| $T_s$ | temperature of motor surface |
| $T_w$ | temperature of winding |
| $T_{EM}$ | electromechanical torque |
| $T_L$ | motor-load torque |
| $U$ | voltage |
| $V$, $V'$, $V^*$ | shaft volume, referenced shaft volume, scaling ratio of shaft volume |
| $x_{sm}$ | displacement of driving part |
| $x_{EMA}$ | displacement of EMA output |
| $\varepsilon$ | surface emissivity |
| $\eta_{EMA}$ | efficiency of the gearbox and the screw mechanism |
| $\theta_G$ | angular position of gearbox |
| $\theta_M$ | motor position |
| $\xi$ | motor damping coefficient |
| $\sigma$ | Stefan's constant |
| $\varphi_m$ | magnetic flux of permanent magnet |
| $\omega_M$ | motor angular velocity |